

Λ_c^+ polarization measurement in pp collisions with the LHCb detector

Elisabeth Maria Niel

GDR annual workshop, 15-17 November 2021

<https://tel.archives-ouvertes.fr/tel-03414369>



Baryon polarization: experimental status

2

- Intriguing results from 90's: strange baryons produced using unpolarized beams were found polarized
 1. 1976: 300 GeV protons on Be target : **polarization up to 28%** [FERMILAB-PUB-76-157-E](#)
 2. 1978: 400 GeV protons on Be target : polarization up to 24% and $\bar{\Lambda}^0$ **polarization zero** [FERMILAB-PUB-78-145-E](#)

Baryon	System	Beam energy [GeV]	Result	p_T range [GeV/c]
1976 Λ^0	$p\text{Be}$	300	18%	1.5
	$p\text{Be}$	400	24%	2.1
	$p\text{C}$ and $p\text{W}$	920	~ 0	~ 0.8
		450	up to 0.29%	0.86
1978 $\bar{\Lambda}^0$	$p\text{Be}$	400	0	up to 1.2
	$p\text{-X}$	400	0	up to 2.4
Ω^-	$p\text{Be}$	800	~ 0	[0.5, 1.3]
1993 Σ^+	$p\text{Cu}$	800	16%	1.0
	$p\text{Cu}$ and $p\text{Be}$	400	$\sim 20\%$	1.6
		800	up to 0.09%	0.76
1990 Ξ^-	$p\text{Be}$	400	up to 10%	1.21
	$p\text{Cu}$	400	up to 0.07%	0.63
	$p\text{Be}$	800	up to 0.1%	>0.8

Features that seem to emerge:

- 
- Increasing polarization with p_T
 - A (not well-defined) target dependence
 - Different polarization between hyperon and anti-hyperon.

Mechanism at the origin of baryons polarization not understood, need new measurements

Motivations: magnetic dipole moments (MDM)

3

The measurement of Λ_c^+ polarization at LHCb is a necessary input for a long-term project aiming at measuring the magnetic dipole moment of charmed baryons

MDM is a fundamental property of particles with spin:

$$\vec{\mu} = \frac{g}{2} \frac{q}{m} \vec{s} \text{ where } g \text{ is the gyromagnetic factor}$$

- For elementary particles, classical prediction $g = 2$. Quantum corrections can slightly modify this value.
- If $g \neq 2$ indication of a composite structure (\rightarrow New Physics)
- Charmed baryons, can be used to measure the **charm quark MDM** $\rightarrow \mu_{\Lambda_c^+} = \mu_c$

Motivations: magnetic dipole moments (MDM)

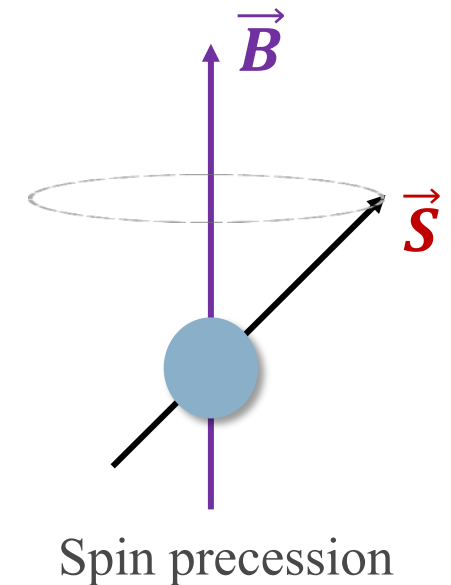
4

The measurement of Λ_c^+ polarization at LHCb is a necessary input for a long-term project aiming at measuring the magnetic dipole moment of charmed baryons

MDM is a fundamental property of particles with spin:

$$\vec{\mu} = \frac{g}{2} \frac{q}{m} \vec{S} \text{ where } g \text{ is the gyromagnetic factor}$$

- For elementary particles, classical prediction $g = 2$. Quantum corrections can slightly modify this value.
- If $g \neq 2$ indication of a composite structure (\rightarrow New Physics)
- Charmed baryons, can be used to measure the **charm quark MDM** $\rightarrow \mu_{\Lambda_c^+} = \mu_c$
- Measured using **spin precession** in a magnetic field
- Method successfully used for *muon MDM* :
g-2 experiment $\rightarrow 4.2 \sigma$ tension with the SM [Phys. Rev. Lett. 126, 141801](#)
- *Tau* (short $c\tau = 87 \mu\text{m}$) \rightarrow no direct measurements
Indirect measurement not precise enough to compare to SM prediction



Magnetic dipole moments (MDM)

Baryons MDM:

- Proton and neutron measured, results in agreement with quark model prediction: $\mu_n^{(a)} = -\frac{2}{3} \mu_p^{(b)}$ (a) [Science. 358 \(6366\): 1081–1084.](#) (b) [Phys. Rev. D. 86 \(1\): 010001.](#)
- For short-lived baryons harder: strong magnetic field required to make precession happen before the decay
→ **need for a new technique**

Magnetic dipole moments (MDM)

6

Baryons MDM:

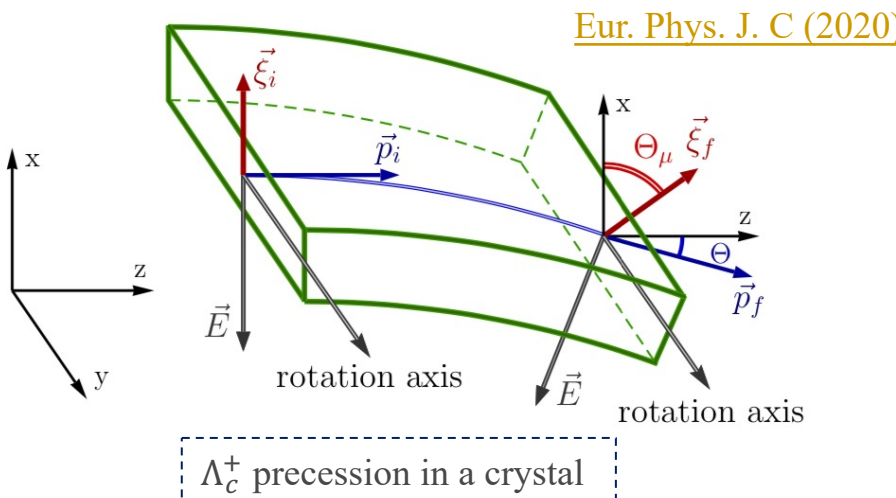
- Proton and neutron measured, results in agreement with quark model prediction: $\mu_n^{(a)} = -\frac{2}{3} \mu_p^{(b)}$
- For short-lived baryons harder: strong magnetic field required to make precession happen before the decay
→ **need for a new technique**

(a) [Science. 358 \(6366\): 1081–1084.](#)

(b) [Phys. Rev. D. 86 \(1\): 010001.](#)

MDM measurement using bent crystals:

- Conventional methods: maximum 45.5 T [Nature 570, 496–499 \(2019\)](#)
- Use strong effective magnetic field produced between crystal planes
- Used for Σ^+ (1990) and promising for charmed baryons [FERMILAB-THESIS-1992-40](#)



$$\vec{\mu} = \frac{g}{2} \frac{q}{m} \vec{s}$$

$$\Theta_\mu \approx \gamma \left(\frac{g}{2} - 1 \right) \Theta$$

Need initial ($\vec{\xi}_i$) and final ($\vec{\xi}_f$) Λ_c^+ polarization

$\vec{\xi}_f$: measured using dedicated experiment or LHCb

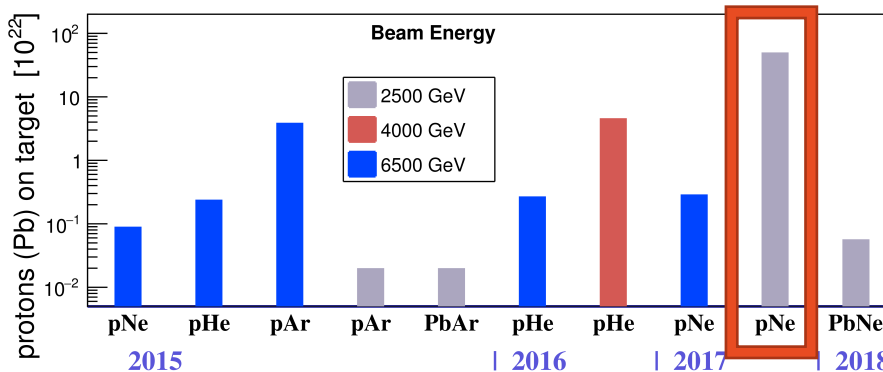
$\vec{\xi}_i$: produce baryons using a *target-crystal* before the bending crystal → measure polarization with LHCb fixed-target sample which has similar condition

The LHCb experiment

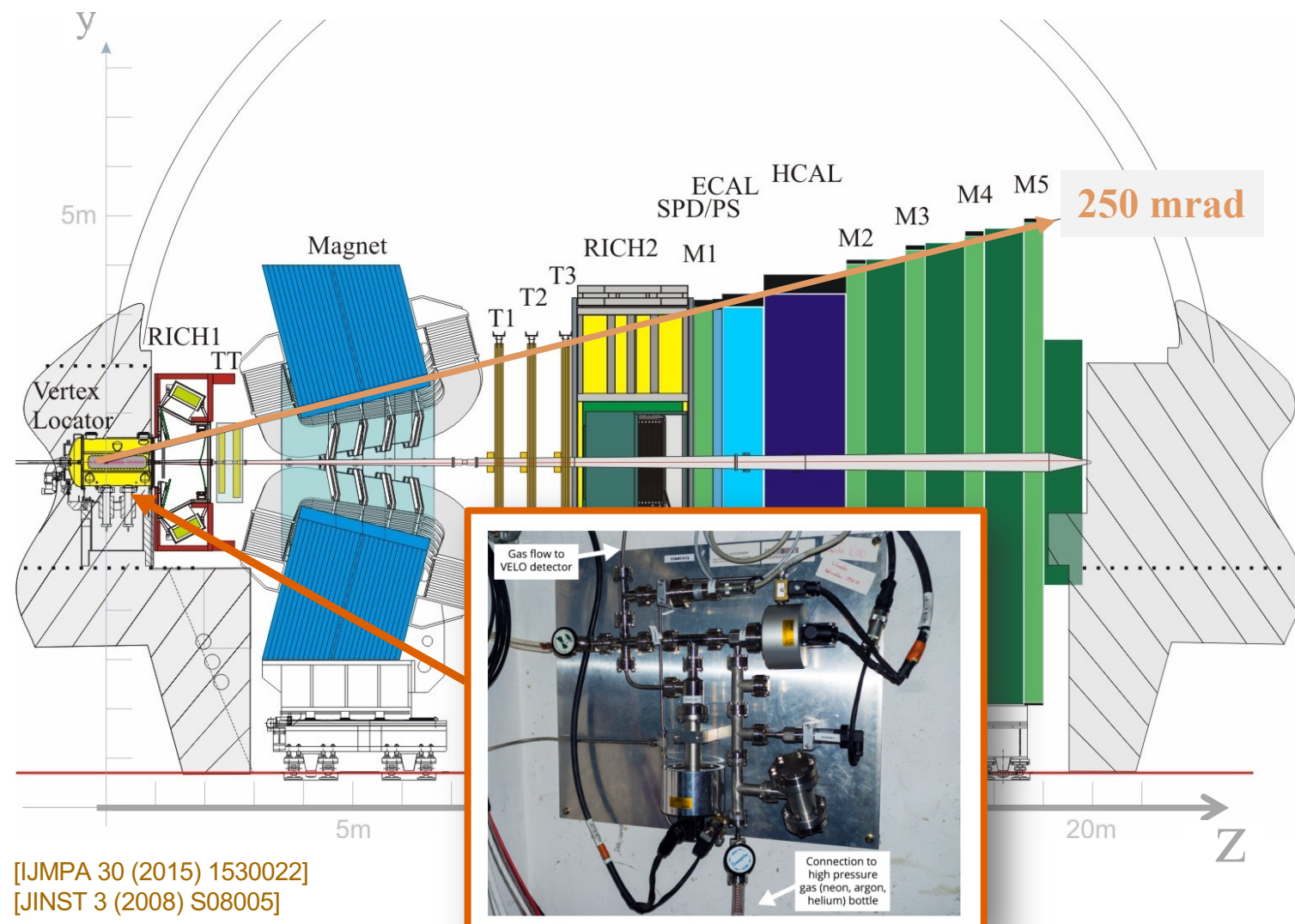
Single arm forward spectrometer: acceptance $2 < \eta < 5$... see description from Valeriia's talk [here](#)

SMOG:

- System for Measuring Overlap with Gas
- Inject tiny quantities of gas inside the VELO tank
- Transforms LHCb in a fixed target experiment



- Unique at the LHC

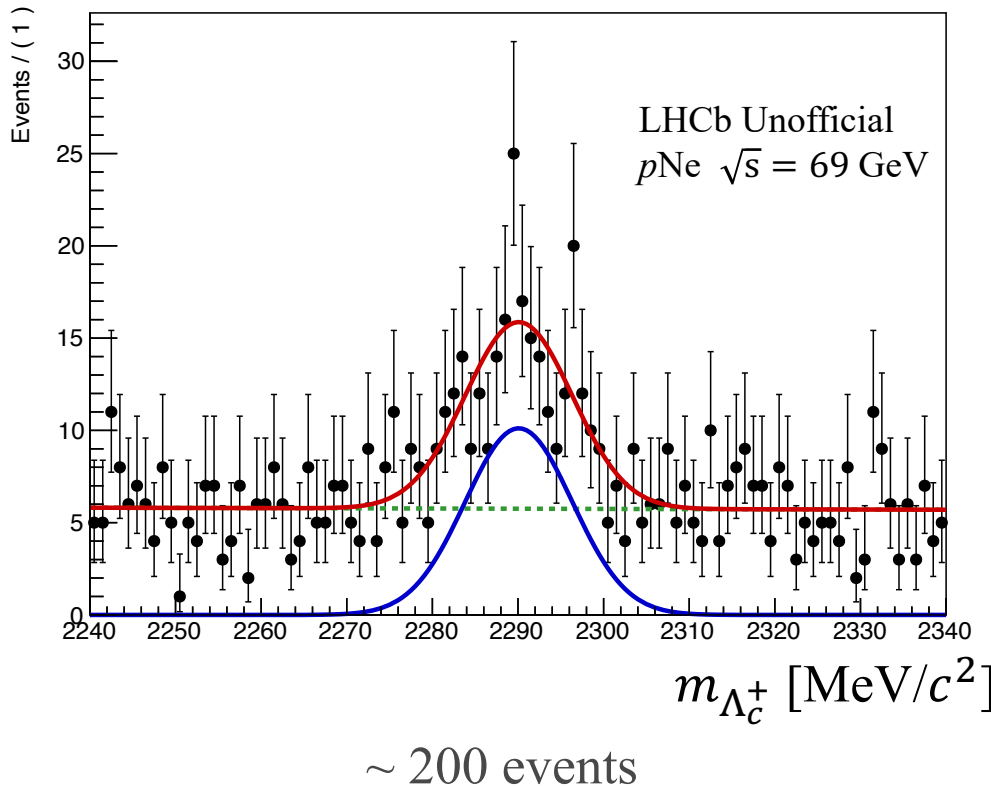


SMOG compared to pp data

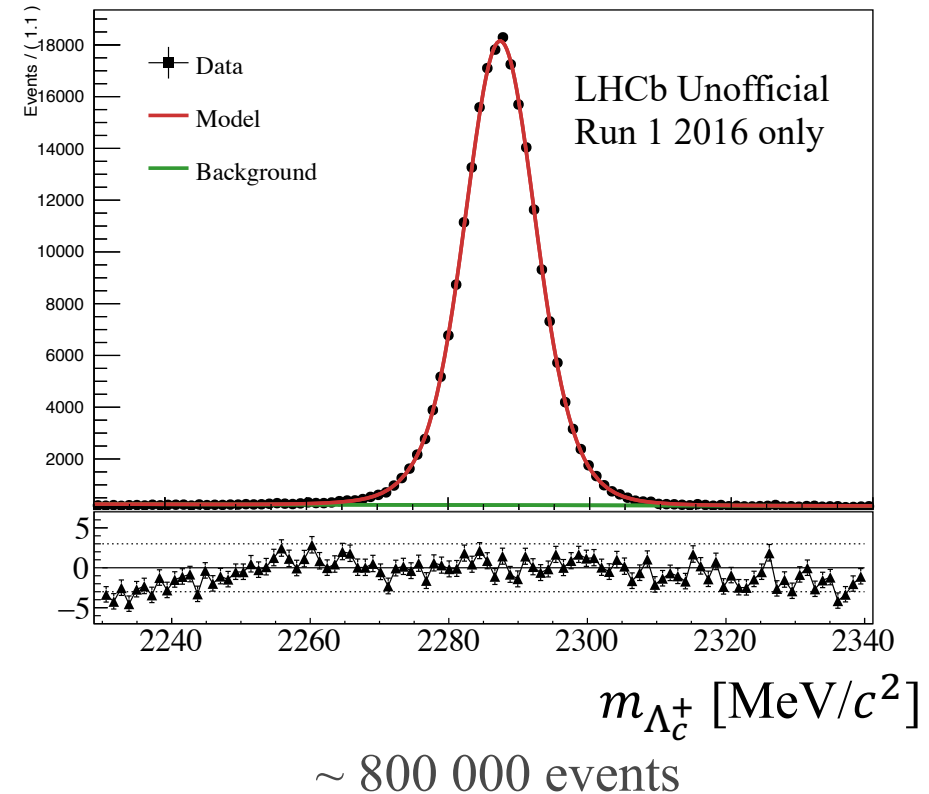
The initial ($\vec{\xi}_i$) Λ_c^+ polarization can be measured in SMOG fixed-target sample.

- LHCb: $p\text{Ne}$ sample at $\sqrt{s} = 69$ GeV, has a similar energy as final set up

Low statistic + pp contamination



Preliminary analysis on the pp sample
to extract a model



Baryon polarization: key concepts

- Polarization of spin $\frac{1}{2}$ baryon: one spin projection ($+1/2 \uparrow$ or $-1/2 \downarrow$) is more likely than the other.
- How to measure it: angular distribution $\Lambda_c^+ \rightarrow X + Y$

$$\frac{1}{N} \frac{d\Gamma}{d\cos\theta} \propto \frac{1}{2} (1 + \alpha \xi \cos\theta)$$

θ : angle baryon momentum and Λ_c^+ spin

ξ : magnitude of the baryon polarization

$$\left\{ \begin{array}{l} \alpha = \frac{2\text{Re}(A_{PV}^* A_{PC})}{|A_{PV}|^2 + |A_{PC}|^2} \\ A_{PV} = \text{parity violating} \\ A_{PC} = \text{parity conserving} \end{array} \right.$$

I. The **decay asymmetry parameter α** : is independent of the production mechanism.

II. The **polarization ξ** instead depends on the production mechanism.

- a. The larger is α the larger is the sensitivity on the polarization
- b. If parity is conserved, $\alpha = 0 \rightarrow$ loss of sensitivity: need a weak decay
- c. If $\xi = 0$, α can only be measured for 3-body decays

Baryon polarization: key concepts

10

- Polarization of spin $\frac{1}{2}$ baryon: one spin projection ($+1/2 \uparrow$ or $-1/2 \downarrow$) is more likely than the other.
- How to measure it: angular distribution $\Lambda_c^+ \rightarrow X + Y$

$$\frac{1}{N} \frac{d\Gamma}{d\cos\theta} \propto \frac{1}{2} (1 + \alpha \xi \cos\theta)$$

θ : angle baryon momentum and Λ_c^+ spin

ξ : magnitude of the baryon polarization

$$\left\{ \begin{array}{l} \alpha = \frac{2\text{Re}(A_{PV}^* A_{PC})}{|A_{PV}|^2 + |A_{PC}|^2} \\ A_{PV} = \text{parity violating} \\ A_{PC} = \text{parity conserving} \end{array} \right.$$

I. The **decay asymmetry parameter α** : is independent of the production mechanism.

II. The **polarization ξ** instead depends on the production mechanism.

- a. The larger is α the larger is the sensitivity on the polarization
- b. If parity is conserved, $\alpha = 0 \rightarrow$ loss of sensitivity: need a weak decay
- c. If $\xi = 0$, α can only be measured for 3-body decays

III. For the 3-body decay $\Lambda_c^+ \rightarrow p K^- \pi^+ \rightarrow$ compute **effective α** using method of M. Davier, et al. Physics Letters B, 306, 3–4, 1993, 411-417
Decompose the amplitude as:

$$\mathcal{P}(\Omega) = f(\Omega) + \xi g(\Omega) = \hat{f}(\Omega)(1 + \xi \omega) \quad \rightarrow \quad S^2 = \left\langle \frac{g^2}{f^2}(\Omega) \right\rangle = \int \frac{g^2}{f^2} d\Omega \quad \rightarrow$$

$$\alpha_{\text{effective}} = \frac{\sqrt{3}}{2} S$$

MDM and the $\Lambda_c^+ \rightarrow p K^- \pi^+$ amplitude analysis

11

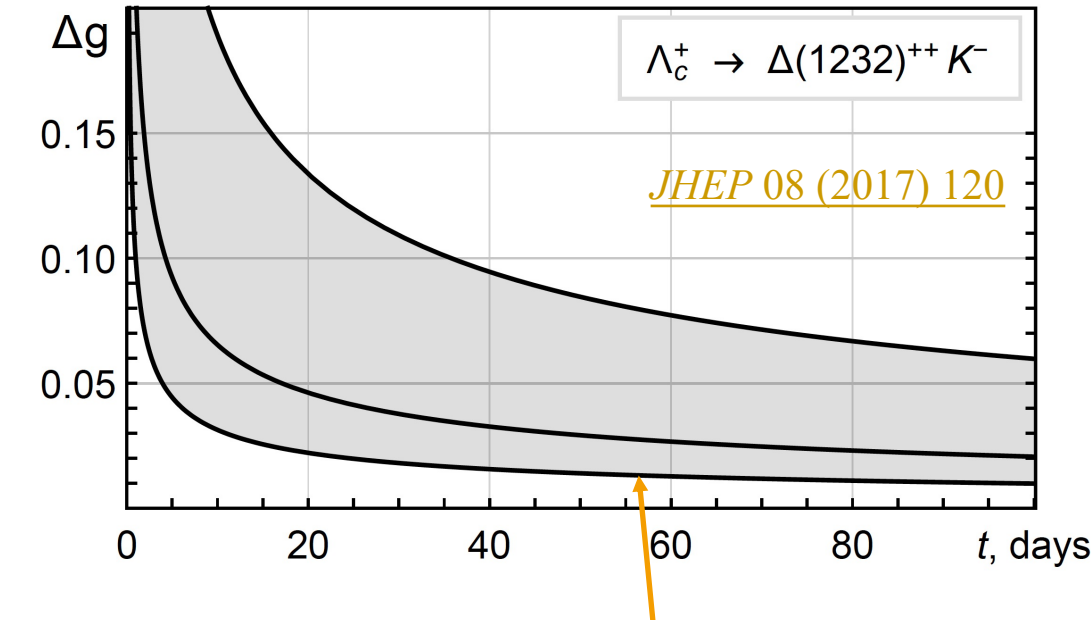
- The error on the gyromagnetic factor is dominated by the knowledge of α and $\vec{\xi}$.

$$\Delta g = \frac{1}{\alpha |\xi|^\Theta} \sqrt{\frac{12}{\Phi t \eta_{\text{det}} \frac{\Gamma_j}{\Gamma} \int \frac{\partial N_{\text{tar+crys}}}{\partial \varepsilon} \gamma^2 d\varepsilon}}.$$

This motivates the analysis of the $\Lambda_c^+ \rightarrow p K^- \pi^+$ decay to measure precisely its properties and the production polarization.

- Previous amplitude analysis of $\Lambda_c^+ \rightarrow p K^- \pi^+$ by E791
Dataset: **1000 Λ_c^+ and $\bar{\Lambda}_c^-$ events**, in 500 GeV/c π -N collisions [Phys.Lett.B471:449-459,2000](#)

Result: *increasing polarization as a function of p_T*
→ the amplitude model used was not correct



After this measurement these error bands will be reduced

LHCb: p Ne sample at $\sqrt{s} = 69$ GeV, has a similar energy as foreseen crystals experiment.

First step: build a model using the higher statistics pp sample.

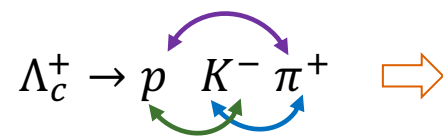
Amplitude analysis of the $\Lambda_c^+ \rightarrow p K^- \pi^+$ decays

1. Introduction to the analysis: physics case
2. Helicity amplitudes: development of the formalism
3. LHCb data analysis

The amplitude

13

- How is the 2-body amplitude modified in the 3-body case? Decompose $\Lambda_c^+ \rightarrow p K^- \pi^+$ in **subsequent decays**



1. $\Lambda_c^+ \rightarrow (K^* \rightarrow K^- \pi^+) p$
2. $\Lambda_c^+ \rightarrow (\Delta^{++} \rightarrow p \pi^+) K^-$
3. $\Lambda_c^+ \rightarrow (\Lambda^* \rightarrow p K^-) \pi^+$

Important differences:

- Each chain can interfere with the others
- Each chain has a large number of resonances

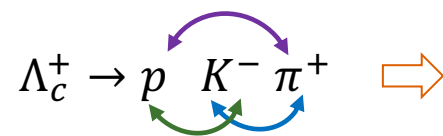
- Isobar decomposition: factorize the amplitude in **angular part** (*helicity amplitudes*) and **dynamic part** (*lineshapes*):

$$\mathcal{A}(\vec{\Omega}) = \sum_i \psi_{r_i}(\vec{\Omega}) \Delta_{r_i}(m_{r_i})$$

The amplitude

14

- How is the 2-body amplitude modified in the 3-body case? Decompose $\Lambda_c^+ \rightarrow p K^- \pi^+$ in **subsequent decays**



1. $\Lambda_c^+ \rightarrow (K^* \rightarrow K^- \pi^+) p$
2. $\Lambda_c^+ \rightarrow (\Delta^{++} \rightarrow p \pi^+) K^-$
3. $\Lambda_c^+ \rightarrow (\Lambda^* \rightarrow p K^-) \pi^+$

Important differences:

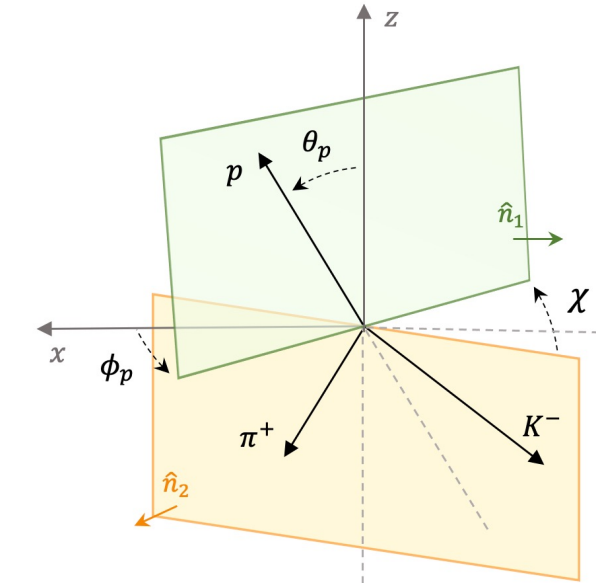
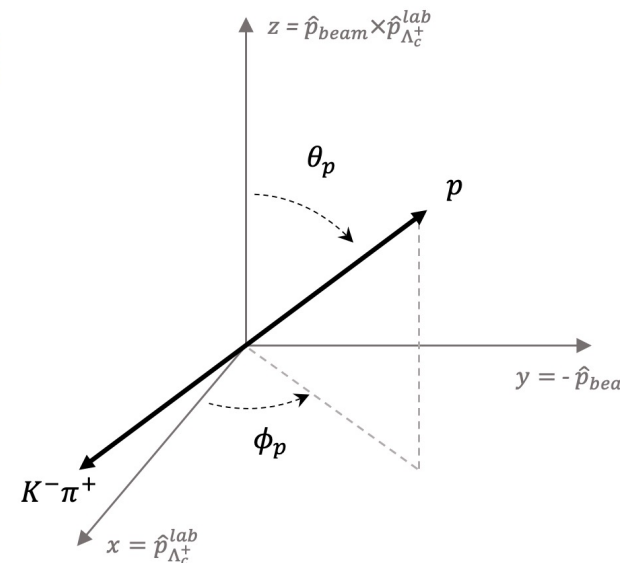
- Each chain can interfere with the others
- Each chain has a large number of resonances

- Isobar decomposition: factorize the amplitude in **angular part (helicity amplitudes)** and **dynamic part (lineshapes)**:

$$\mathcal{A}(\vec{\Omega}) = \sum_i \psi_{r_i}(\vec{\Omega}) \Delta_{r_i}(m_{r_i})$$

- Kinematics of $\Lambda_c^+ \rightarrow p K^- \pi^+$ described by 5 variables :

- $m_{p\pi}^2 = (P_p + P_\pi)^2$ and $m_{pK}^2 = (P_p + P_K)^2$
- (θ_p, ϕ_p) : polar and azimuthal angle of the proton at Λ_c^+ rest frame
- χ : angle between the planes formed by the proton direction and the z axis and K^- and π^+ directions

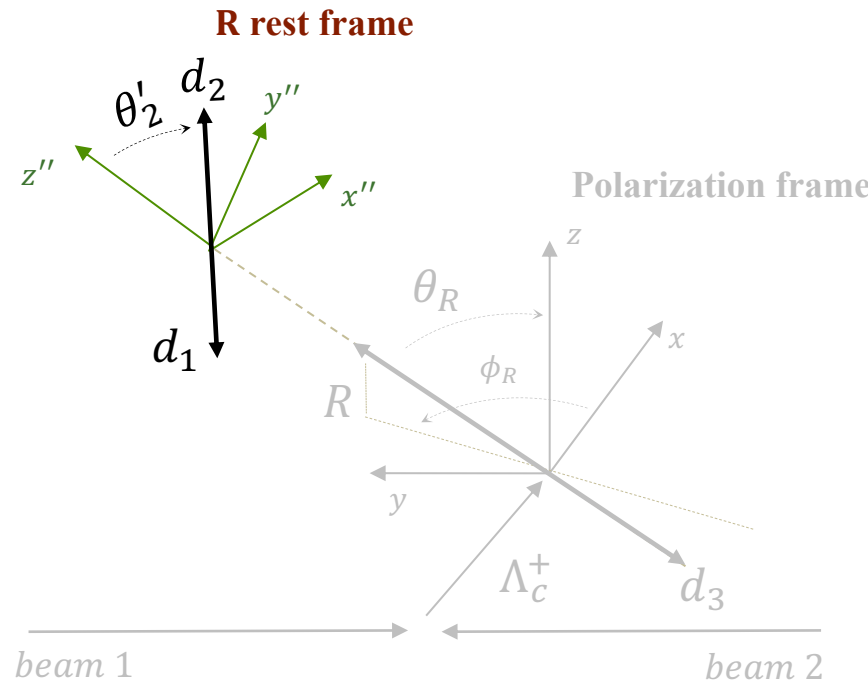


The 3 Euler angles give the orientation of the plane.
Polarization may introduce a non-trivial angular dependence.

Helicity formalism

15

Helicity operator: invariance under rotations and boosts along \hat{p} : $\Lambda = \frac{\vec{J} \cdot \vec{p}}{\|\vec{p}\|} = (\vec{L} + \vec{S}) \cdot \hat{\mathbf{p}} = \vec{S} \cdot \hat{\mathbf{p}}$



Resonance (R) rest frame

- Reached by means of a **rotation + boost**.
- The new z axis is aligned to the resonance momentum in the polarization frame.
- Do it for each chain:
 1. $\Lambda_c^+ \rightarrow (K^* \rightarrow K^- \pi^+) p$
 2. $\Lambda_c^+ \rightarrow (\Delta^{++} \rightarrow p \pi^+) K^-$
 3. $\Lambda_c^+ \rightarrow (\Lambda^* \rightarrow p K^-) \pi^+$

The total amplitude: spin matching

16

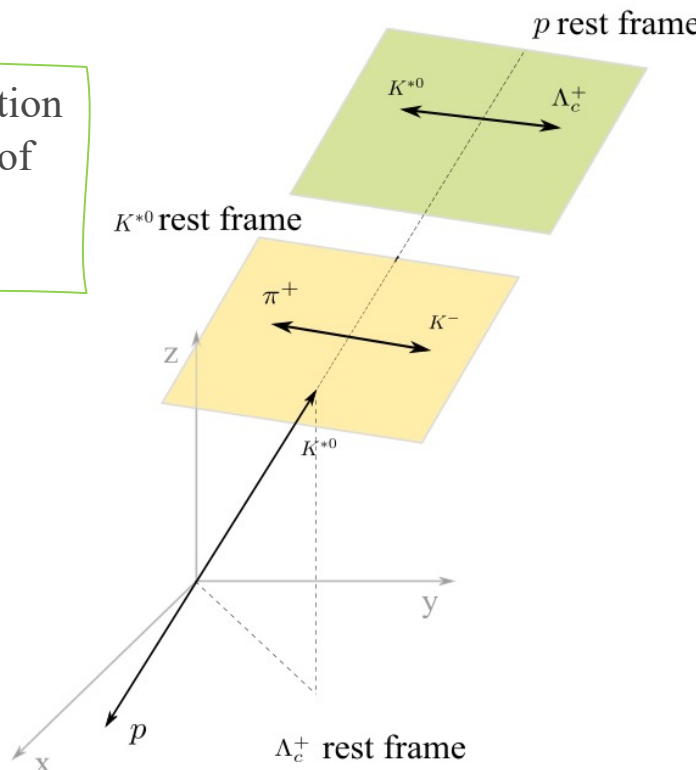
Need to add the 3 chains passing through different paths.

Definition of the helicity changes depending on the path used to reach the helicity frame (of the proton):

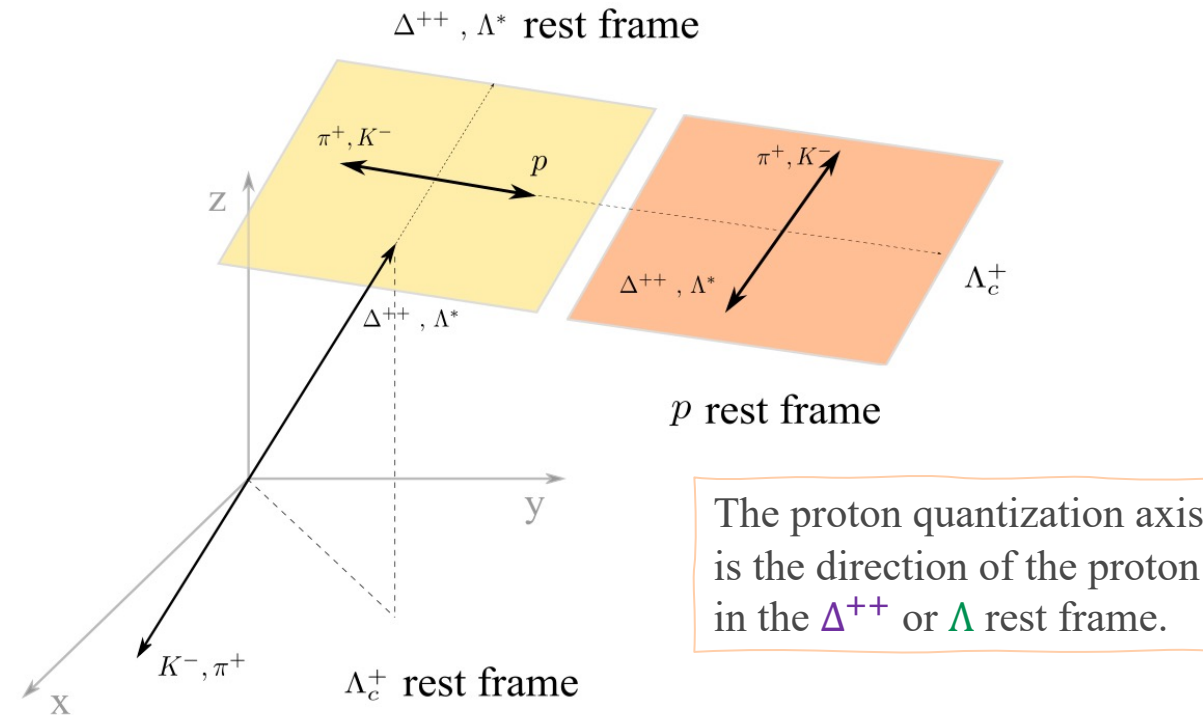
1. $\Lambda_c^+ \rightarrow$ Res helicity frame
2. Res helicity frame \rightarrow proton helicity frame

$$\Lambda_c^+ \rightarrow (K^* \rightarrow K^- \pi^+) p$$

The proton quantization axis is the direction of the proton in the Λ_c^+ rest frame



$$\Lambda_c^+ \rightarrow (\Delta^{++} \rightarrow p\pi^+) K^- \text{ and } \Lambda_c^+ \rightarrow (\Lambda^* \rightarrow pK^-) \pi^+$$



The proton quantization axis is the direction of the proton in the Δ^{++} or Λ^* rest frame.

The total amplitude

17

- Need: **Wigner rotation** to align the proton projection axis (see backup).

$$\mathcal{A}_{m,\lambda_p}(\Omega) = \mathcal{A}_{m,\lambda_p}^{K^*}(\Omega_{K^*}) + \sum_{\lambda'_p} \mathcal{A}_{m,\lambda'_p}^{\Lambda^*}(\Omega_{\Lambda^*}) D(\alpha_1, \beta_{\Lambda^*}, \phi'_{K^-}) + \sum_{\lambda'_p} \mathcal{A}_{m,\lambda'_p}^{\Delta^{++}}(\Omega_{\Delta^{++}}) D(\alpha_2, \beta_{\Delta^*}, \phi'_{K^-})$$

$$\alpha_1 = \begin{cases} 2\pi & \text{if } |\phi_p - \phi_\pi| > \pi \\ 0 & \text{else} \end{cases} \quad \alpha_2 = \begin{cases} 2\pi & \text{if } |\phi_p - \phi_K| > \pi \\ 0 & \text{else} \end{cases}$$

- Polarization included via spin density matrix:

$$\rho = \frac{1}{2} (\mathcal{I} + \vec{P} \cdot \vec{\sigma}) = \frac{1}{2} \begin{pmatrix} 1 + P_z & P_x - iP_y \\ P_x + iP_y & 1 - P_z \end{pmatrix}$$

$$\begin{aligned} \mathcal{A}_{m,\lambda_p} = & \sum_s \sum_{\lambda_{K^*0}} B_s(M_{K\pi}) \times D_{\lambda_{K^*0},0}^{s*}(\phi'_K, \theta'_K, 0) D_{m,\lambda_{K^*0}-\lambda_p}^{\frac{1}{2}*}(\phi_{K^*0}, \theta_{K^*0}, 0) b a_{\lambda_{K^*0}, \lambda_p} \\ & + \sum_s \sum_{\lambda'_p, \lambda_{\Delta^{++}}} B_s(M_{p\pi}) \times D_{\lambda'_p, \lambda_p}(\alpha_2, \beta_{\Delta^{++}}, \phi'_K) D_{\lambda_{\Delta^{++}}, -\lambda'_p}^{s*}(\phi'_\pi, \theta'_\pi, 0) D_{m, \lambda_{\Delta^{++}}}^{\frac{1}{2}*}(\phi_{\Delta^{++}}, \theta_{\Delta^{++}}, 0) d_{\lambda'_p} c_{\lambda_{\Delta^{++}}} \\ & + \sum_s \sum_{\lambda'_p, \lambda_{\Lambda^*}} B_s(M_{pK}) \times D_{\lambda'_p, \lambda_p}(\alpha_1, \beta_{\Lambda^*}, \phi'_K) D_{\lambda_{\Lambda^*}, \lambda'_p}^{s*}(\phi'_p, \theta'_p, 0) D_{m, \lambda_{\Lambda^*}}^{\frac{1}{2}*}(\phi_{\Lambda^*}, \theta_{\Lambda^*}, 0) f_{\lambda'_p} e_{\lambda_{\Lambda^*}} \end{aligned}$$

$$d\Gamma \sim \sum_{m,m'} \rho_{m,m'} \sum_{\lambda_p} A_{m,\lambda_p} A_{m',\lambda_p}^*$$

N.B.: The Wigner rotation contains a "**2π factor**" ($\alpha_{1,2}$) to compensate for the fact that a 2π rotation does not leave the system invariant.

$$D^j(0, 0, 2\pi) = (-1)^{2j} \longrightarrow \text{For } j = \pm \frac{1}{2} \text{ a minus sign arises}$$

Benchmark tests

18

Tests used to check the amplitude formalism and assess the necessity of the Wigner rotations and 2π factor

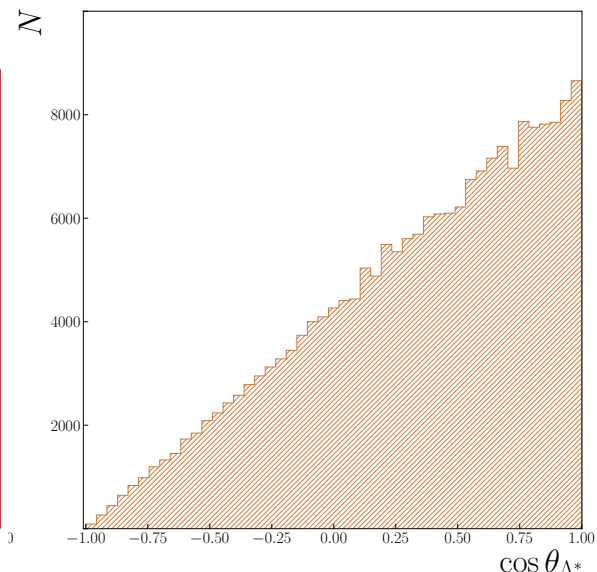
1. **Linearity:** if only one chain is included, the angular distribution must be linear:

Example for the Λ^* chain:

$$\frac{d\Gamma}{d\cos\theta} \sim \frac{4}{3} \left(1 + P_{\Lambda_c} \alpha_{\Lambda_c}^{\Lambda^*} \cos\theta_{\Lambda^*} \right)$$

where

$$\alpha_{\Lambda_c}^{\Lambda^*} = \frac{|H_{1/2,0}^{\Lambda_c^+ \rightarrow \Lambda^* \pi^+}|^2 - |H_{-1/2,0}^{\Lambda_c^+ \rightarrow \Lambda^* \pi^+}|^2}{|H_{1/2,0}^{\Lambda_c^+ \rightarrow \Lambda^* \pi^+}|^2 + |H_{-1/2,0}^{\Lambda_c^+ \rightarrow \Lambda^* \pi^+}|^2} :$$



Decomposition in the angular momentum basis (LS-basis)

$$\begin{cases} h_{\frac{1}{2},0}^{\Lambda_c^+ \rightarrow \Lambda^* \pi^+} = -\sqrt{\frac{1}{2}}(h_{PC}^{\Lambda^*} + h_{PV}^{\Lambda^*}) \\ h_{-\frac{1}{2},0}^{\Lambda_c^+ \rightarrow \Lambda^* \pi^+} = -\sqrt{\frac{1}{2}}(h_{PC}^{\Lambda^*} - h_{PV}^{\Lambda^*}) \end{cases}$$

$$\alpha_{\Lambda_c}^{\Lambda^*} = -2 \frac{\text{Re}\{h_{PC}^{\Lambda^*} h_{PV}^{\Lambda^* *}\}}{|h_{PC}^{\Lambda^*}|^2 + |h_{PV}^{\Lambda^*}|^2}$$

Non zero asymmetry parameter \rightarrow need both parity violating (PV) and parity conserving (PC) amplitudes

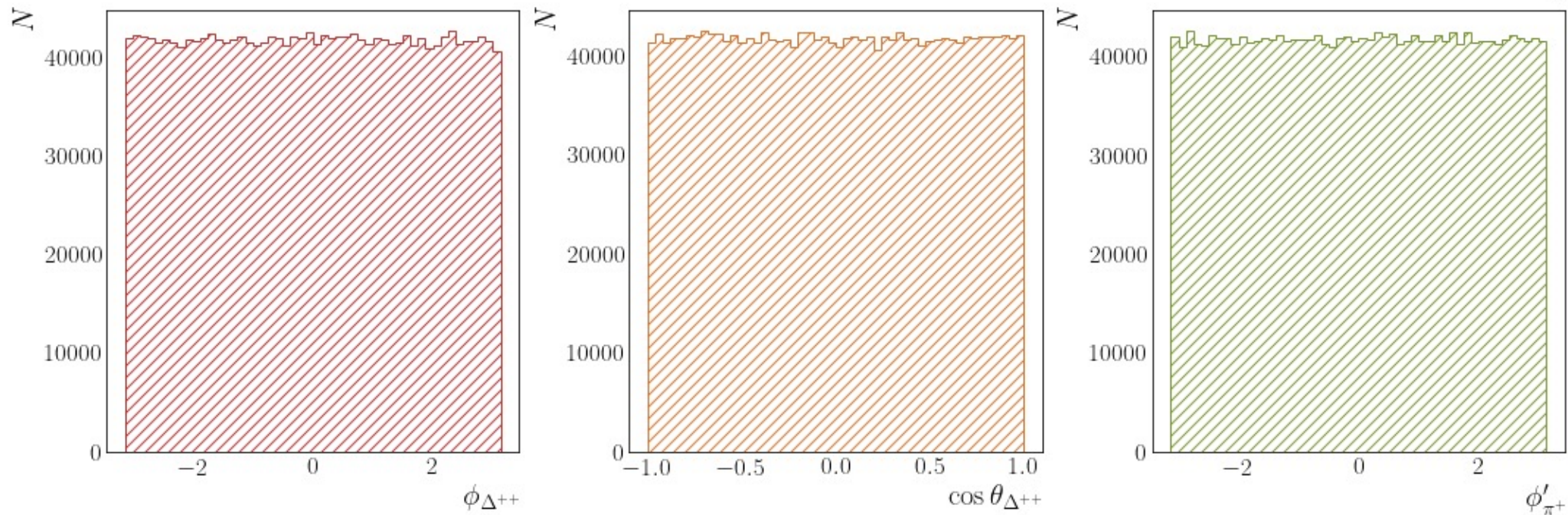
Benchmark tests

19

1. If $P = 0 \rightarrow$ the angular dependence drops
2. If parity conservation enforced for the Λ_c^+ decay $\rightarrow \alpha_{\Lambda_c^+} = 0$

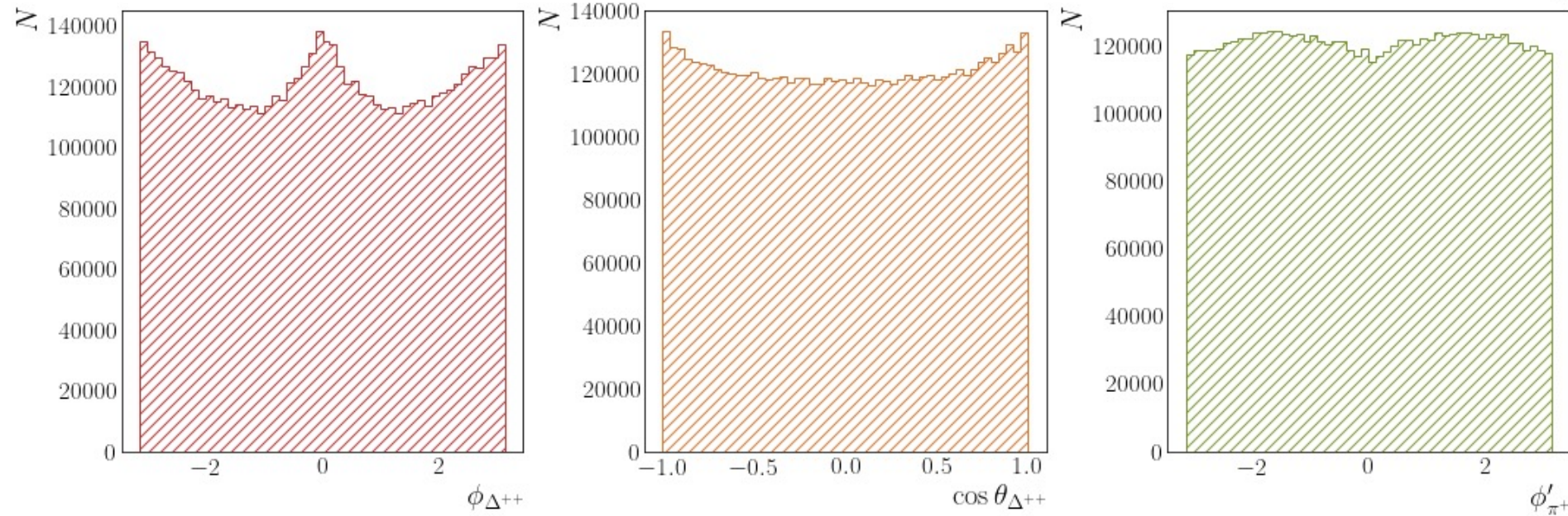


angular distributions
should be flat



Example : Δ^{++} chain angles

Test used to assess the need of the azimuthal part of the Wigner rotation,
Without Wigner rotation and 2π condition the angular distributions are not flat



Example : Δ^{++} chain angles, without including the 2π condition

Amplitude analysis of the $\Lambda_c^+ \rightarrow p K^- \pi^+$ decays

1. Introduction to the analysis: physics case
2. Helicity amplitudes: development of the formalism
3. LHCb data analysis

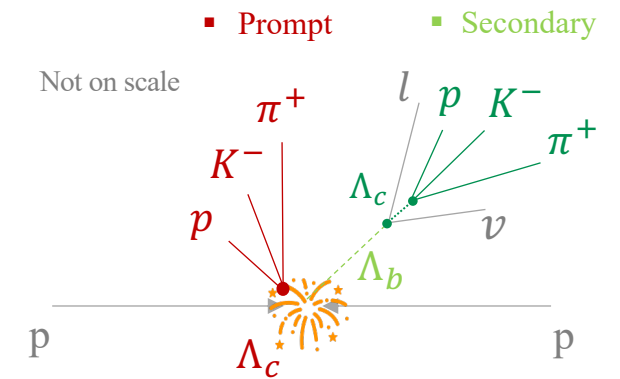
Introduction

22

Goal: measure polarization for promptly produced (i.e. not from B decays) Λ_c^+ in pp collisions using the LHCb detector

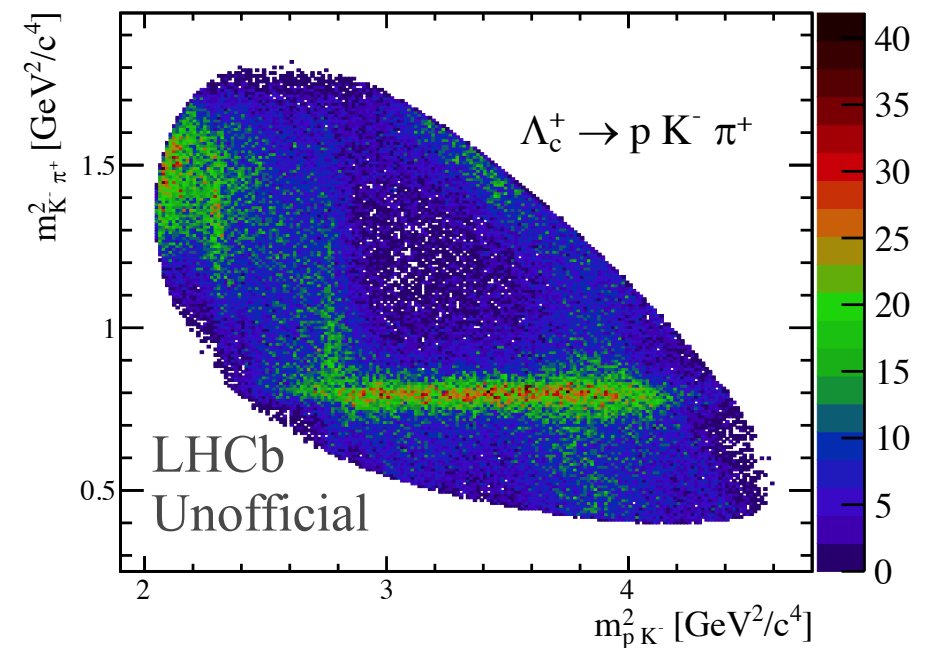
How: amplitude analysis of the decay mode $\Lambda_c^+ \rightarrow p K^- \pi^+$

Sample: LHCb Run 2 (only 2016), pp collisions at $\sqrt{s} = 13$ TeV



Analysis strategy

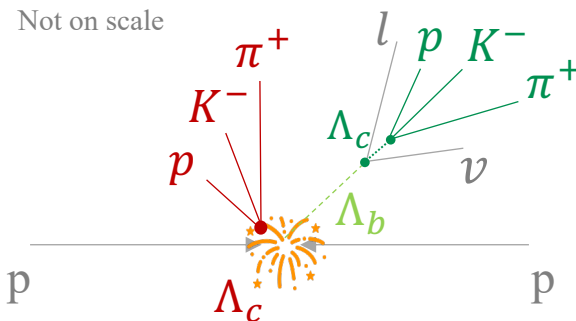
1. Select signal events to obtain a high purity prompt sample
2. Use the amplitude formalism obtained to fit the data:
 - a) Build a model: assess the presence of resonances
 - b) 5 dimensional unbinned likelihood fit
 - c) Systematic studies



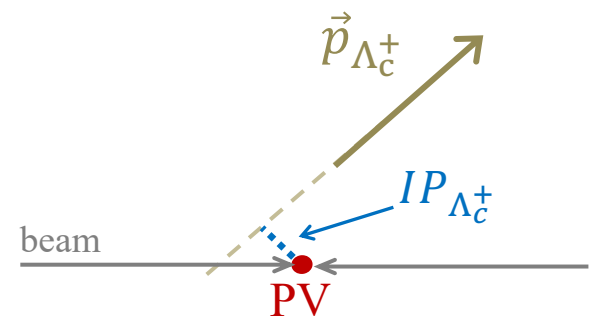
Signal selection

23

- Low background, mainly misidentification and combinatorial (backup)
- Most important selection: separation prompt/secondary



Different polarization since
different production mechanism



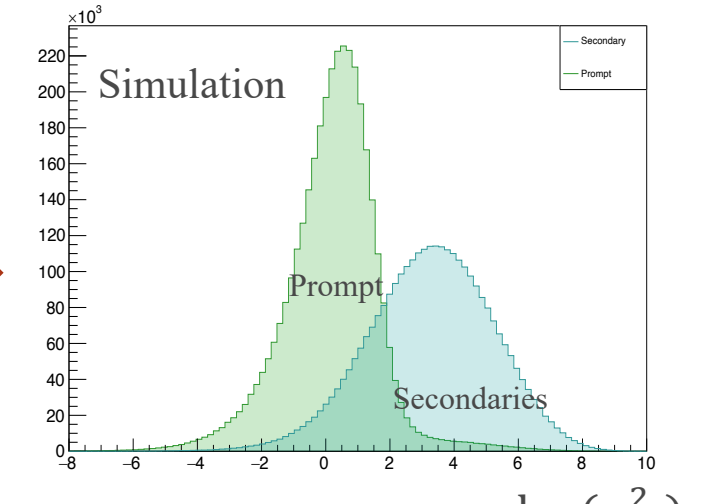
Quantity used: impact parameter

- Signal purity evaluated in $\log(\chi_{IP}^2)$ the range [-6,6]

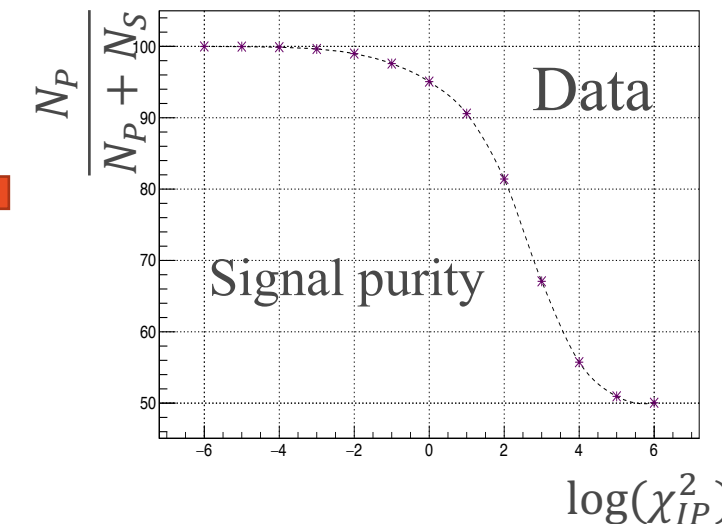
Final selection:

$$\log(\chi_{IP}^2) < -2.$$

Prompt signal purity: 98.9 %



$\log(\chi_{IP}^2)$



$\log(\chi_{IP}^2)$



↓

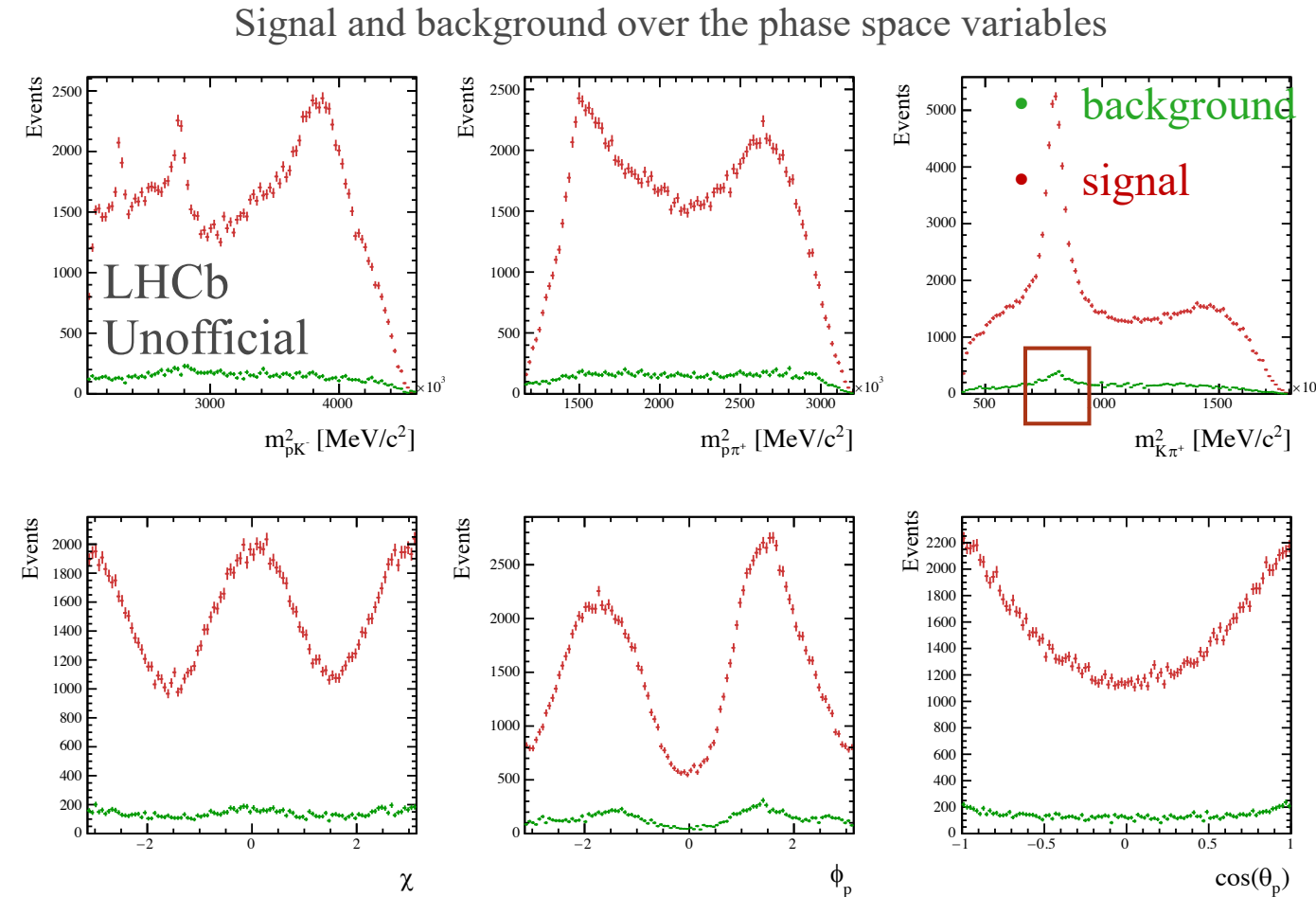
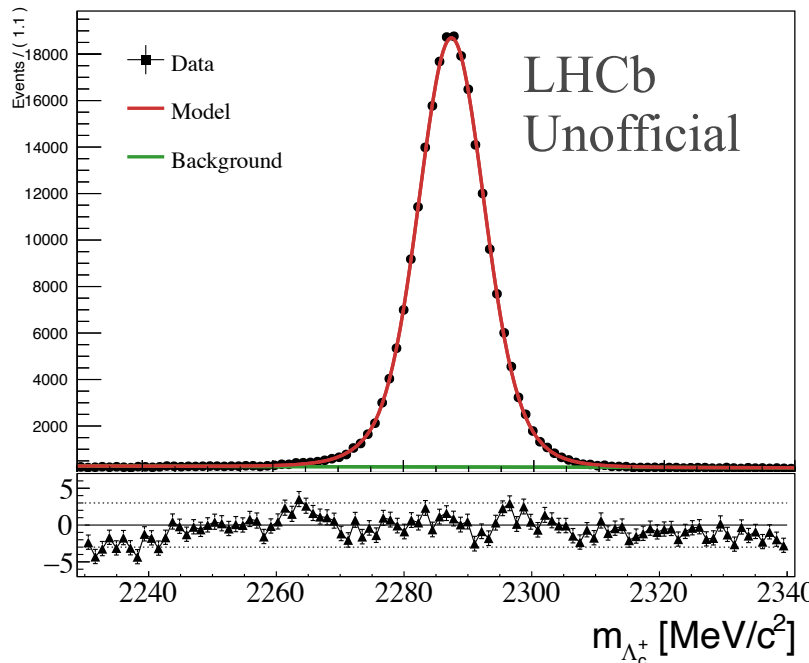


Signal selection

24

- Low background, mainly misidentification and combinatorial (backup)
- Most important selection: separation prompt/secondary
- Residual background taken into account using *sPlot technique*

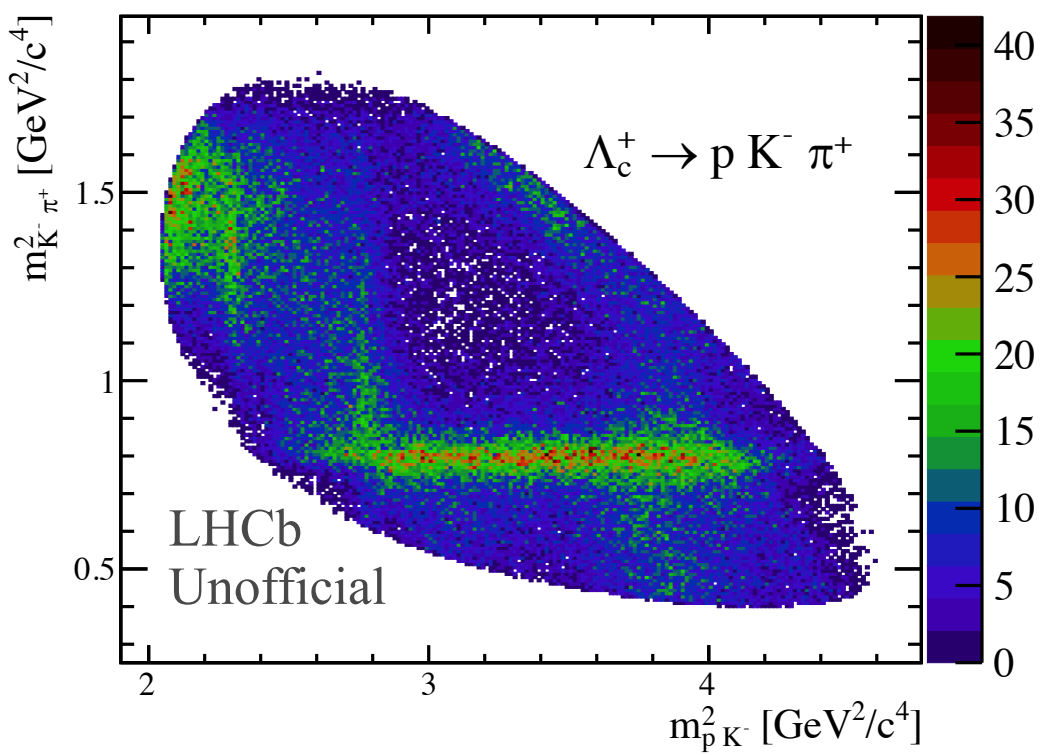
Fit after selections: signal purity $\sim 97\%$



Model choice for amplitude fit

25

- List of known resonances large, all possibly contributing
- Model building: assess which resonances contribute to the fit
- Strategy:
 1. Add resonances which are visible by eye

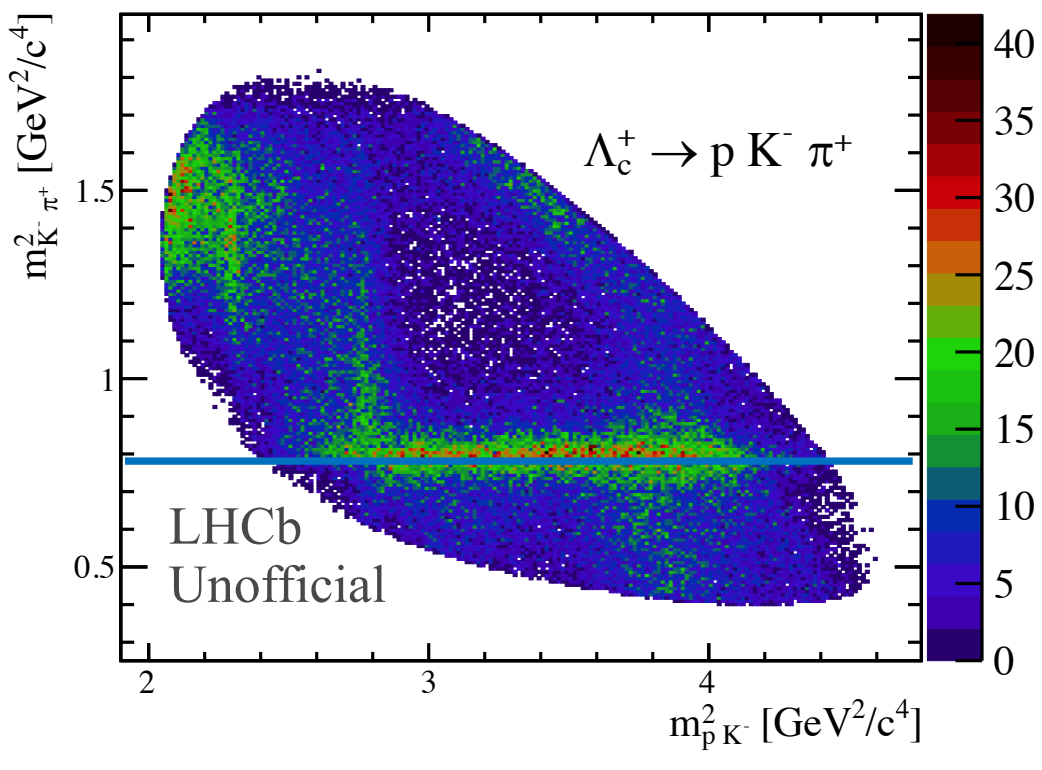


List of known resonances		
Particle	J^P	Overall status
$\Lambda(1116)$	$1/2^+$	****
$\Lambda(1380)$	$1/2^-$	**
$\Lambda(1405)$	$1/2^-$	****
$\Lambda(1520)$	$3/2^-$	****
$\Lambda(1600)$	$1/2^+$	****
$\Lambda(1670)$	$1/2^-$	****
$\Lambda(1690)$	$3/2^-$	****
$\Lambda(1710)$	$1/2^+$	*
$\Lambda(1800)$	$1/2^-$	***
$\Lambda(1810)$	$1/2^+$	***
$\Lambda(1820)$	$5/2^+$	****
$\Lambda(1830)$	$5/2^-$	****
$\Lambda(1890)$	$3/2^+$	****
$\Lambda(2000)$	$1/2^-$	*
Particle	J^P	overall
$\Delta(1232)$	$3/2^+$	****
$\Delta(1600)$	$3/2^+$	****
$\Delta(1620)$	$1/2^-$	****
$\Delta(1700)$	$3/2^-$	****
$\Delta(1750)$	$1/2^+$	*
$\Delta(1900)$	$1/2^-$	***
$\Delta(1905)$	$5/2^+$	****
$\Delta(1910)$	$1/2^+$	****
$\Delta(1920)$	$3/2^+$	***
$\Delta(1930)$	$5/2^-$	***

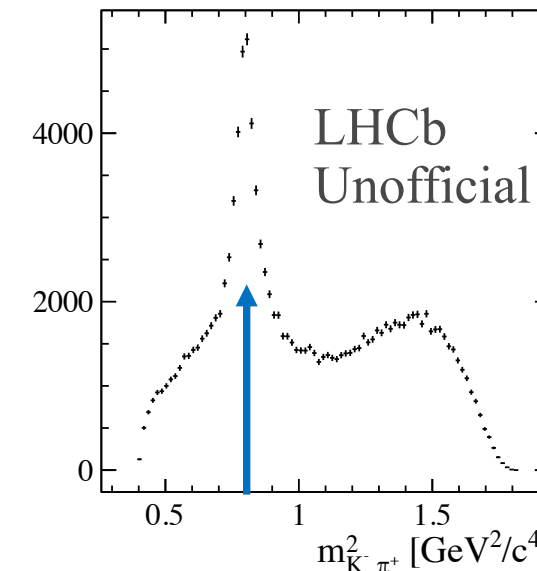
Model choice

26

- List of known resonances large, all possibly contributing
- Model building: assess which resonances contribute to the fit
- Strategy:
 1. Add resonances which are visible by eye



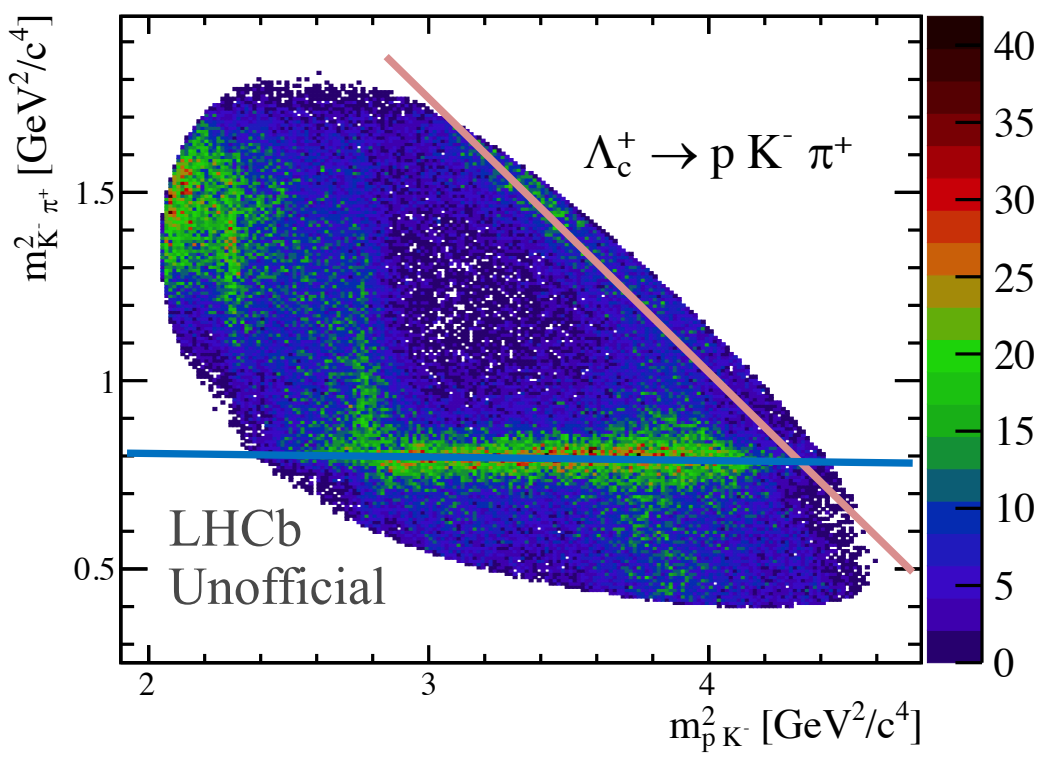
1. $\Lambda_c^+ \rightarrow (K^* \rightarrow K^- \pi^+) p$:
➤ $K^{*0}(890)$



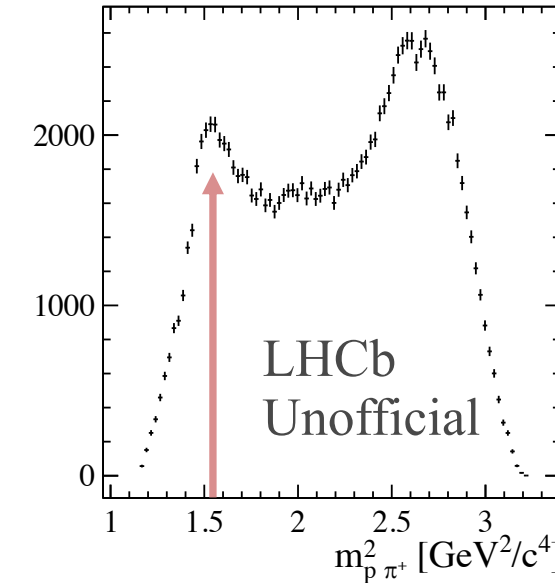
Model choice

27

- List of known resonances large, all possibly contributing
- Model building: assess which resonances contribute to the fit
- Strategy:
 1. Add resonances which are visible by eye



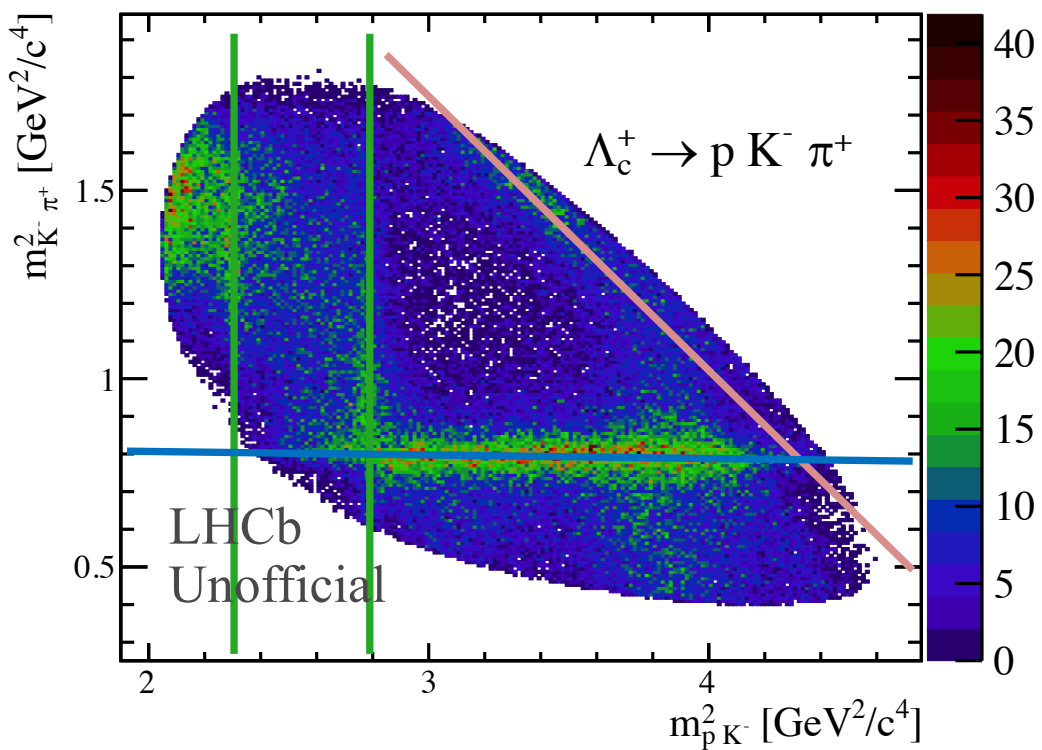
1. $\Lambda_c^+ \rightarrow (K^* \rightarrow K^- \pi^+) p:$
 - $K^{*0}(890)$
2. $\Lambda_c^+ \rightarrow (\Delta^{++} \rightarrow p \pi^+) K^-:$
 - $\Delta^{++}(1232)$



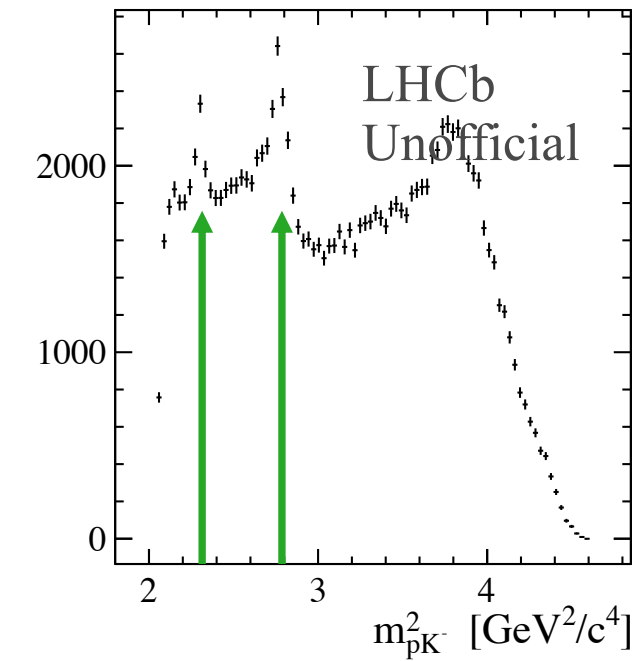
Model choice

28

- List of known resonances large, all possibly contributing
- Model building: assess which resonances contribute to the fit
- Strategy:
 1. Add resonances which are visible by eye



1. $\Lambda_c^+ \rightarrow (K^* \rightarrow K^-\pi^+) p:$
 - $K^{*0}(890)$
2. $\Lambda_c^+ \rightarrow (\Delta^{++} \rightarrow p\pi^+) K^-:$
 - $\Delta^{++}(1232)$
3. $\Lambda_c^+ \rightarrow (\Lambda^* \rightarrow pK^-) \pi^+:$
 - $\Lambda^*(1520)$
 - $\Lambda^*(1670)$



Model choice

- List of known resonances large, all possibly contributing
- Model building: assess which resonances contributes to the fit. Strategy:
 1. Add resonances which are visible by eye
 2. **Model building**, add resonances **iteratively**:

Model choice

- List of known resonances large, all possibly contributing
- Model building: assess which resonances contributes to the fit. Strategy:
 1. Add resonances which are visible by eye
 2. **Model building**, add resonances **iteratively**:
 - Fix polarization to zero → angles have no influence
 - For each model 4 fits with randomized initial values
 - Compare χ^2/ndf : the smallest value preferred

$$\chi^2/\text{ndf} = \frac{1}{N - N_{\text{par}} - 1} \sum_i^N \frac{\text{data}[i] - \text{model}[i]}{\text{err}_{\text{data}}[i]^2 + \text{err}_{\text{model}}[i]^2}$$

Model choice

- List of known resonances large, all possibly contributing
- Model building: assess which resonances contributes to the fit. Strategy:
 1. Add resonances which are visible by eye
 2. **Model building**, add resonances **iteratively**:
 - Fix polarization to zero → angles have no influence
 - For each model 4 fits with randomized initial values
 - Compare χ^2/ndf : the smallest value preferred

$$\chi^2/ndf = \frac{1}{N - N_{par} - 1} \sum_i^N \frac{data[i] - model[i]}{err_{data}[i]^2 + err_{model}[i]^2}$$

In total **25 models** tested → 3 models retained

Res	M0	M1	M2	M3	M4	M5	M6
<i>pK</i> channel							
$\Lambda^*(1405)$	✗	✓	✓	✓	✓	✓	✓
$\Lambda^*(1520)$	✓	✓	✓	✓	✓	✓	✓
$\Lambda^*(1600)$	✗	✗	✓	✓	✓	✓	✓
$\Lambda^*(1670)$	✓	✓	✓	✓	✓	✓	✓
$\Lambda^*(1690)$	✗	✗	✗	✗	✗	✗	✗
$\Lambda^*(1800)$	✗	✗	✗	✗	✗	✗	✗
$\Lambda^*(1810)$	✗	✗	✗	✗	✗	✗	✗
$\Lambda^*(1820)$	✗	✗	✗	✗	✗	✗	✗
$\Lambda^*(1830)$	✗	✗	✗	✗	✗	✗	✗
$\Lambda^*(1890)$	✗	✗	✗	✗	✗	✗	✗
$\Lambda^*(2000)$	✗	✓	✓	✓	✓	✓	✓
$\Lambda^*(2100)$	✗	✗	✗	✗	✗	✗	✗
$\Lambda^*(2110)$	✗	✗	✗	✗	✗	✗	✗
<i>pπ</i> channel							
$\Delta^{++}(1232)$	✓	✓	✓	✓	✓	✓	✓
$\Delta^{++}(1600)$	✗	✗	✗	✗	✓	✓	✓
$\Delta^{++}(1620)$	✗	✗	✗	✗	✗	✗	✓
$\Delta^{++}(1700)$	✗	✗	✗	✗	✗	✓	✓
<i>Kπ</i> channel							
$K^*(700)$	✗	✗	✗	✓	✓	✓	✓
$K^*(892)$	✓	✓	✓	✓	✓	✓	✓
$K^*(1410)$	✗	✗	✗	✗	✗	✗	✗
$K_0^*(1430)$	✗	✗	✗	✓	✓	✓	✓
Fit χ^2/ndf							
N_{par}	18	26	30	34	38	42	46
m_{pK}^2	217.17	40.66	9.18	10.80	12.18	12.30	11.85
$m_{K\pi}^2$	27.27	25.15	12.32	12.43	14.72	13.31	11.60
$m_{p\pi}^2$	55.82	22.64	10.60	12.24	12.50	11.82	11.12
$\cos(\theta_p)$	7.50	6.48	6.28	6.62	7.20	7.73	8.19
χ	6.59	5.44	5.50	5.57	6.35	6.68	7.05
ϕ_p	6.27	5.52	6.08	6.04	6.56	7.19	8.09
$m_{pK}^2, m_{p\pi}^2$	389.18	29.97	7.32	10.38	11.86	11.80	5.04
FF	1.030	0.932	1.100	1.030	1.119	1.102	1.129

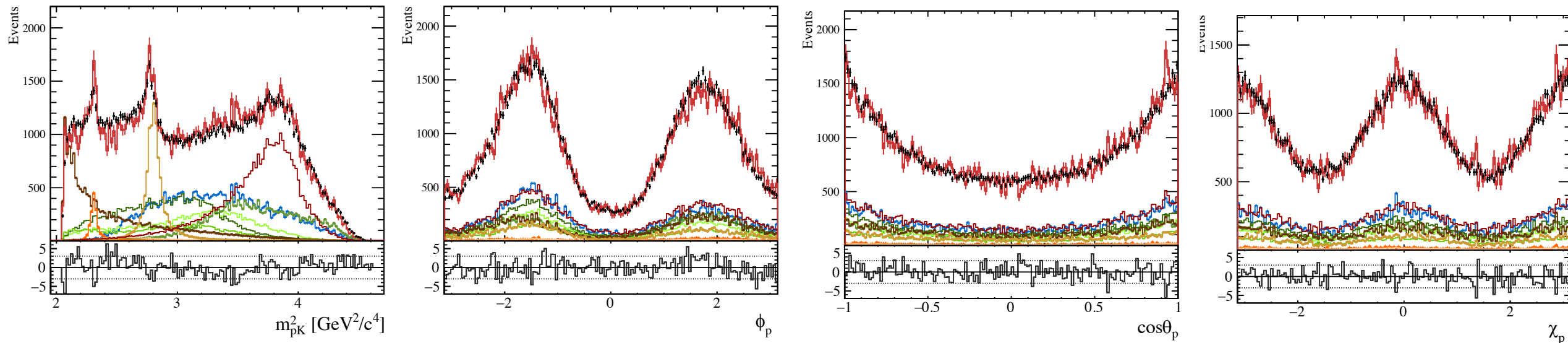
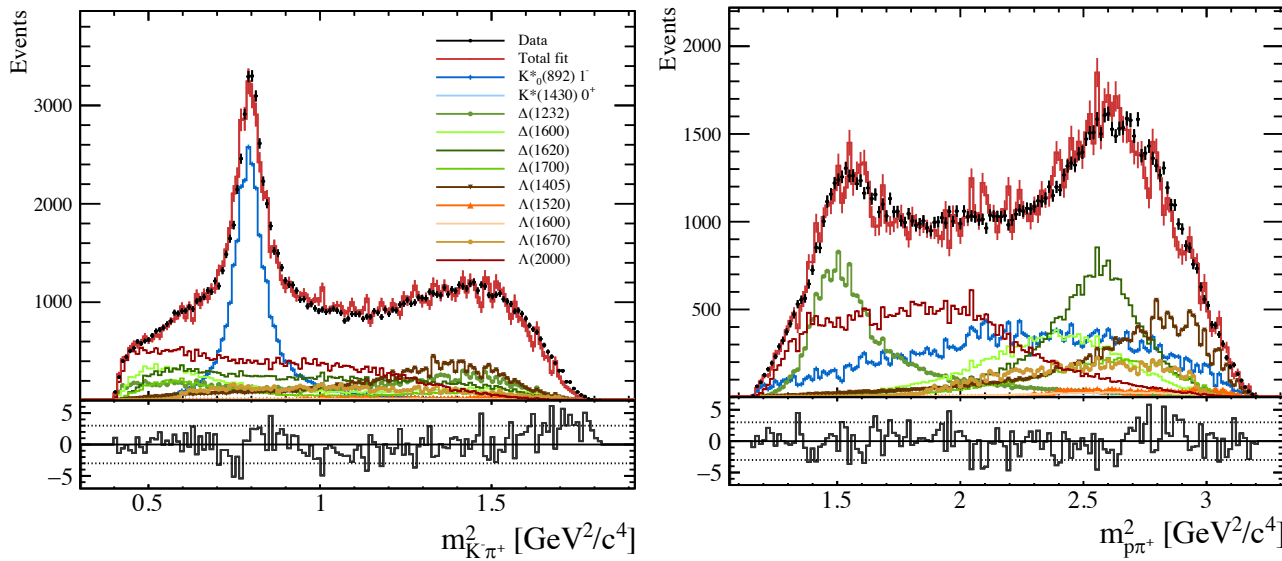


Nominal Model

32

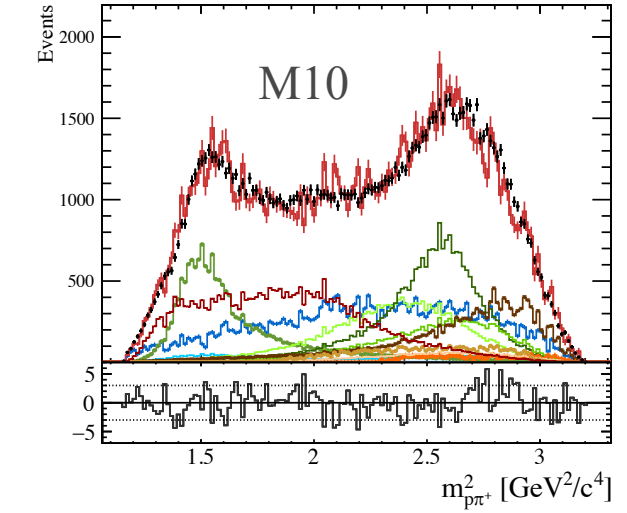
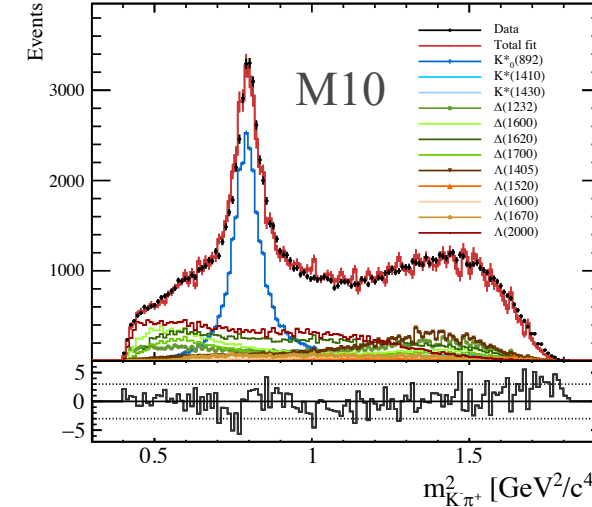
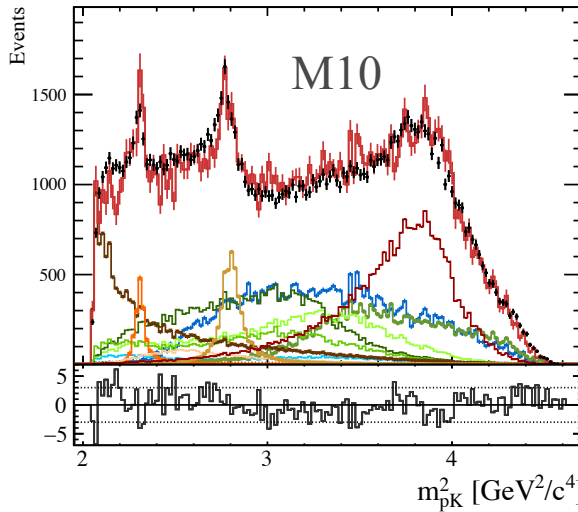
The nominal model is (M6)

- Resonances:
 1. $K^{*0}(700), K^{*0}(890), K^{*0}(1430)$
 2. $\Delta^{++}(1232), \Delta^{++}(1600), \Delta^{++}(1620), \Delta^{++}(1700)$
 3. $\Lambda^*(1405), \Lambda^*(1520), \Lambda^*(1600), \Lambda^*(1670), \Lambda^*(2000)$
- $\sum FF = 1.13$ and $\chi^2/ndf = 5.04$
- Number of parameters 46

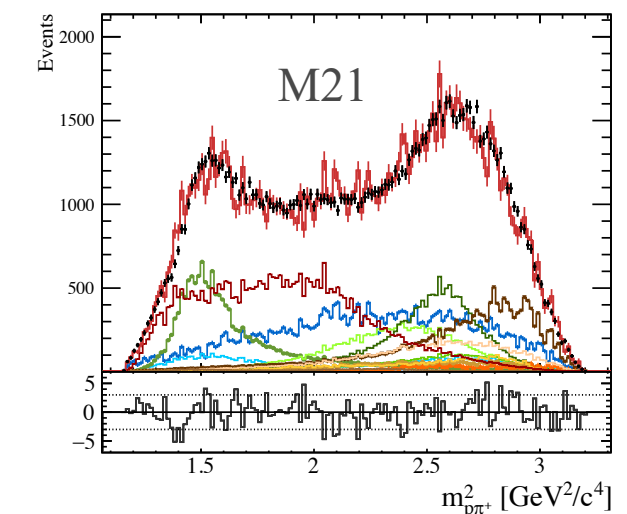
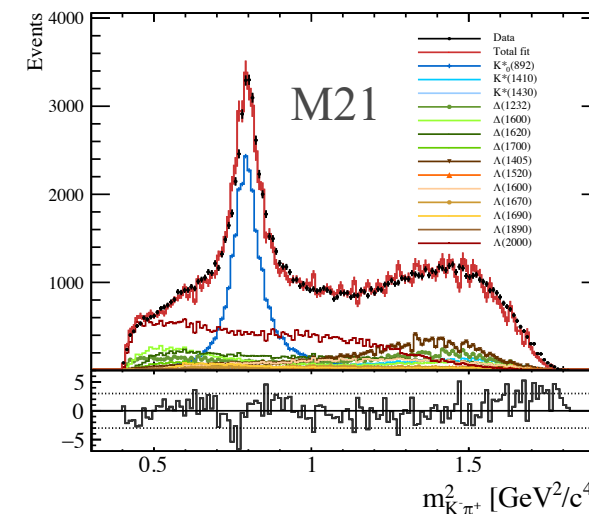
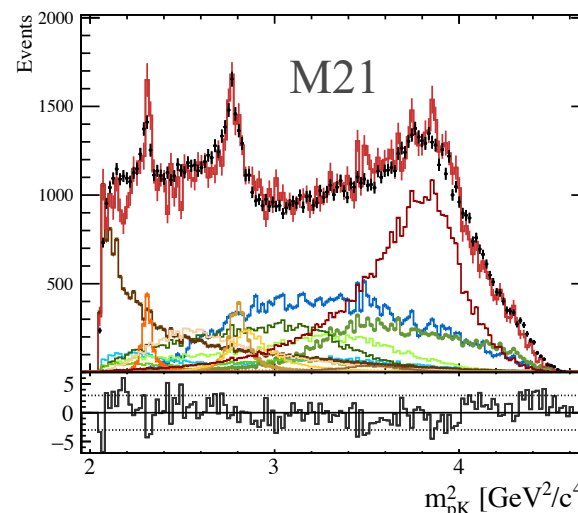


Alternative models

- M10: $M6 + K^{*0}(1410)$



- M21: $M10 + \Lambda^*(1690) \Lambda^*(1890)$



Different fit categories:

- ✓ Λ_c^+ and $\bar{\Lambda}_c^-$, can have different polarizations
- ✓ Magnet polarities (Up and Down), different reconstruction efficiencies in LHCb
- ✓ Trigger categories (L0 hardware trigger): **TOS** and **TIS**, different efficiency effects on ϕ_p angle



8 categories in total, fit separately

Reminder

TOS = Triggered On Signal

TIS = Triggered Independent of Signal

Results shown for one category: negative polarity, TIS trigger category, $\Lambda_c^+ \rightarrow p K^- \pi^+$ decays

	MagDown		MagUp	
MC	TIS	TOS	TIS	TOS
Λ_c^+	34 646	27 686	35 680	27 158
$\bar{\Lambda}_c^-$	34 398	28 523	34 488	28 643
Data	TIS	TOS	TIS	TOS
Λ_c^+	110 720	73 783	105 426	65 866
$\bar{\Lambda}_c^-$	108 394	78 340	104 852	70 295

Across all sample at least **96 % signal purity**
and ~1% of secondary contamination

Results

35

- Fit fractions and effective asymmetry parameter ($\alpha_{effective}$) are shown.
The helicity couplings are degenerate for zero polarization, values not shown.
- Results shown for one category: negative polarity, TIS trigger, $\Lambda_c^+ \rightarrow p K^- \pi^+$ decays
- Statistical error $\sim 0.6\%$:
- Model choice dominates the systematic uncertainty. Larger systematics on the polarization around 9 %

$$P_x = -0.0233 \pm (0.0046)_{stat} \pm (0.0341)_{sys}$$

$$P_y = 0.0560 \pm (0.0044)_{stat} \pm (0.0919)_{sys}$$

$$P_z = 0.0095 \pm (0.0063)_{stat} \pm (0.0590)_{sys}$$

$$\alpha_{effective} = 0.715 \pm 0.005$$

Reminder

$$\alpha_{effective} = \frac{\sqrt{3}}{2} S$$

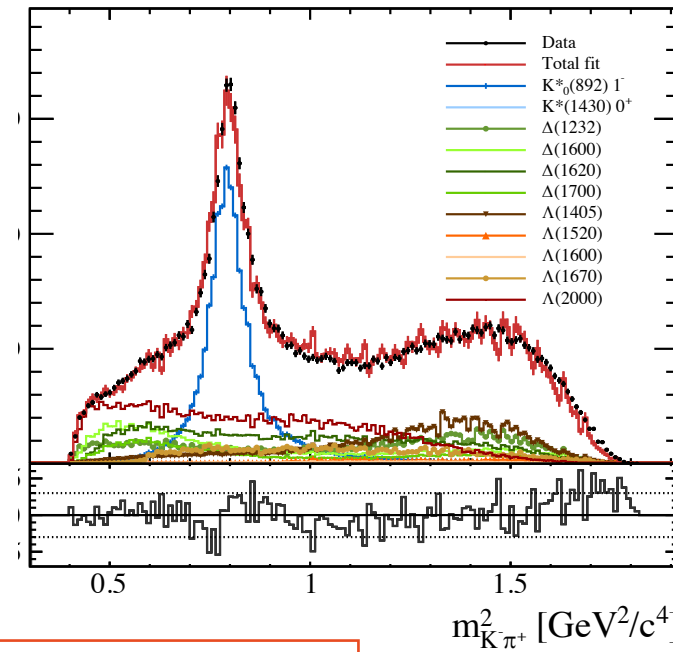
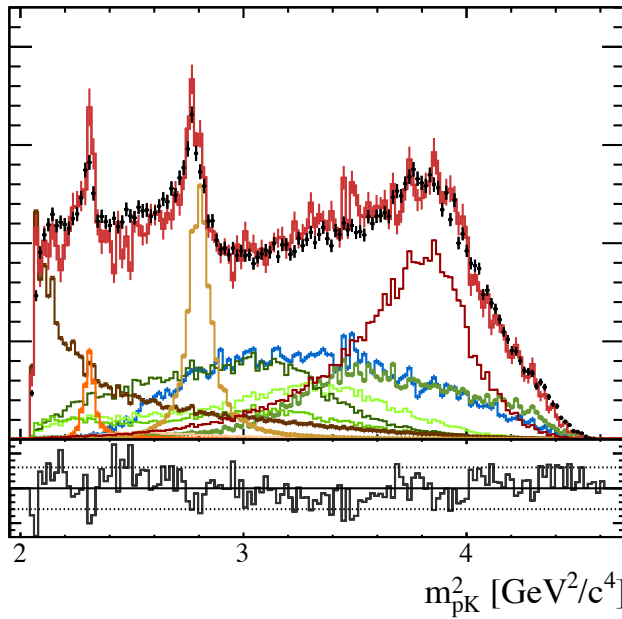
FF parameter	Central value	Statistical uncertainty
$\Delta^{++}(1232)$	0.12245	0.00011
$\Delta^{++}(1600)$	0.08202	0.00009
$\Delta^{++}(1620)$	0.15003	0.00454
$\Delta^{++}(1700)$	0.04804	0.00043
$K^*(1430)$	0.00322	0.00005
$K^*(890)$	0.19532	0.00012
$\Lambda^*(1405)$	0.19201	0.00056
$\Lambda^*(1520)$	0.03197	0.00011
$\Lambda^*(1600)$	0.00738	0.00009
$\Lambda^*(1670)$	0.06240	0.00059
$\Lambda^*(2000)$	0.22201	0.00036
$\sum F_{ri}$	1.11685	0.00706

Conclusions

Conclusions and prospects

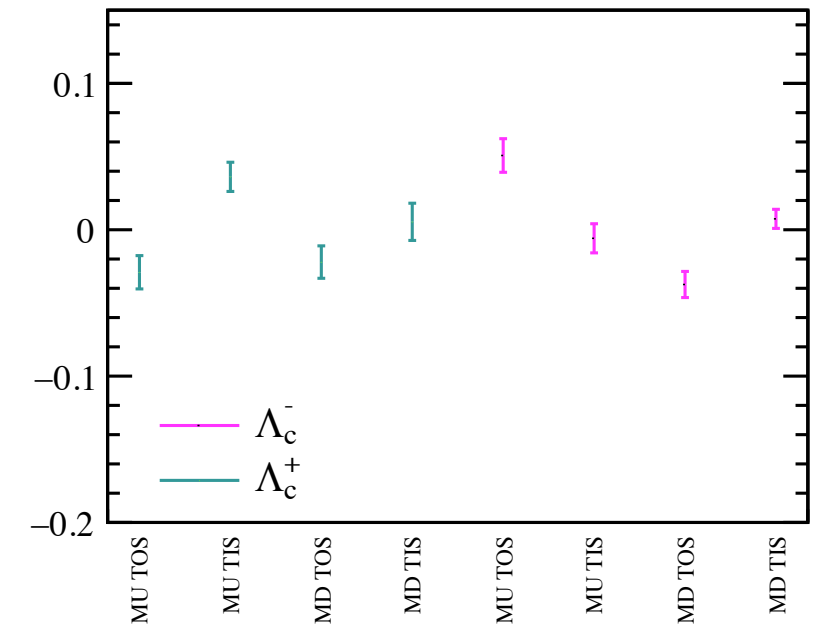
37

- We measured the polarization of prompt produced Λ_c^+ baryons by mean of a 5-dimensional amplitude analysis of the 3-body decay $\Lambda_c^+ \rightarrow p K^- \pi^+$
- The result is dominated by the systematic uncertainty (around 6 % for P_z)



Paper under preparation and expected soon.

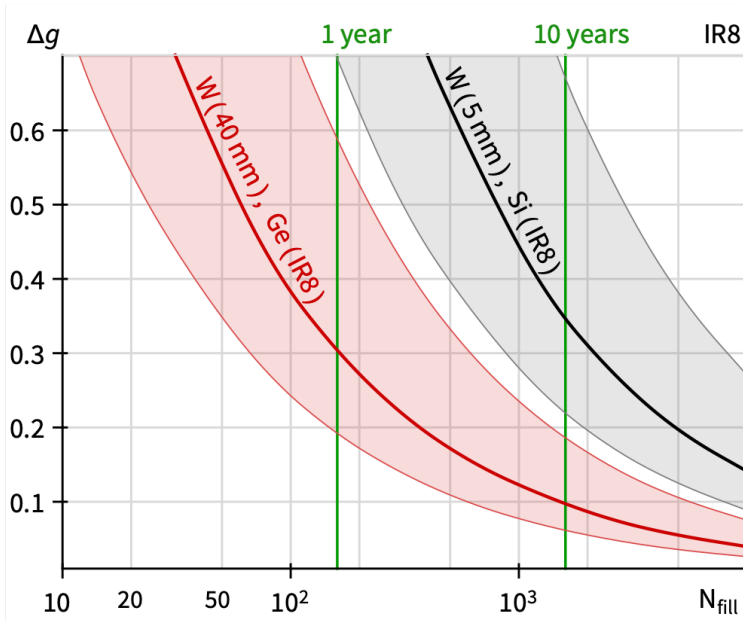
Results for different categories → compatible within maximum 2 σ



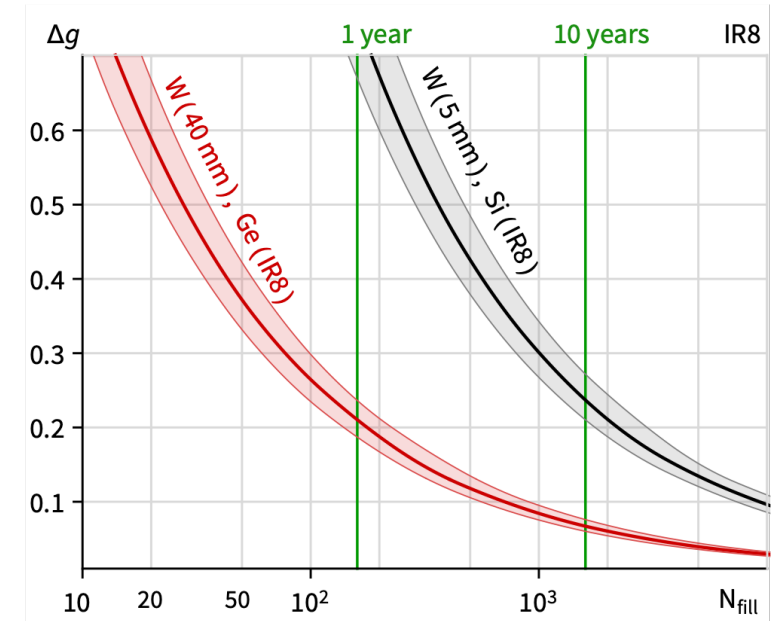
Conclusions and prospects

38

- We measured the polarization of prompt produced Λ_c^+ baryons by mean of a 5-dimensional amplitude analysis of the 3-body decay $\Lambda_c^+ \rightarrow p K^- \pi^+$
- The result is dominated by the systematic uncertainty (around 6 % for P_z)
- The large measured value of $\alpha_{effective}$ prove that the $\Lambda_c^+ \rightarrow p K^- \pi^+$ decay can be used to measure the polarization in the context of the MDM experiments using crystals.



Improvement thanks to
the knowledge of α



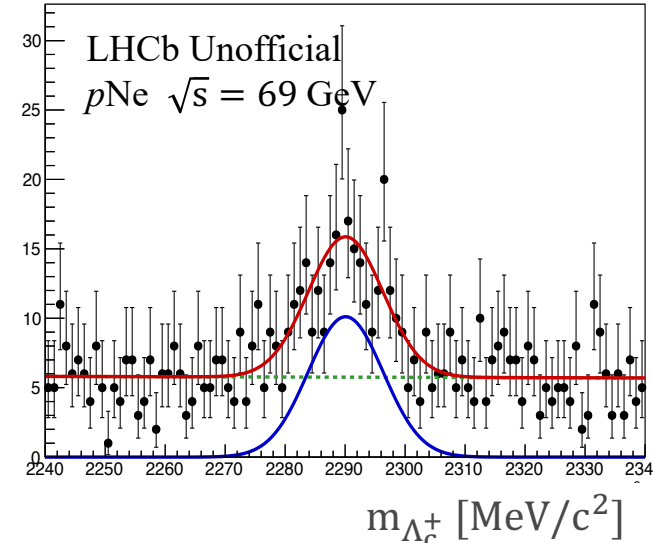
Conclusions and prospects

39

- We measured the polarization of prompt produced Λ_c^+ baryons by mean of a 5-dimensional amplitude analysis of the 3-body decay $\Lambda_c^+ \rightarrow p K^- \pi^+$
- The result is dominated by the systematic uncertainty (around 6 % for P_z)
- The large measured value of $\alpha_{effective}$ prove that the $\Lambda_c^+ \rightarrow p K^- \pi^+$ decay can be used to measure the polarization in the context of the MDM experiments using crystals.

Prospects:

- The equations and the technique developed can be used in other amplitude analysis e.g. $\Xi_c^+ \rightarrow p K^- \pi^+$. What about higher spin baryons?
- The model obtained will be used to measure Λ_c^+ polarization in the fixed-target sample:
 - estimated statistical uncertainty for current SMOG sample: 10 – 14 %
 - SMOG2: would allow to reduce the statistical uncertainty to 0.4 %, the measurement will be limited by the systematic error due to the model choice

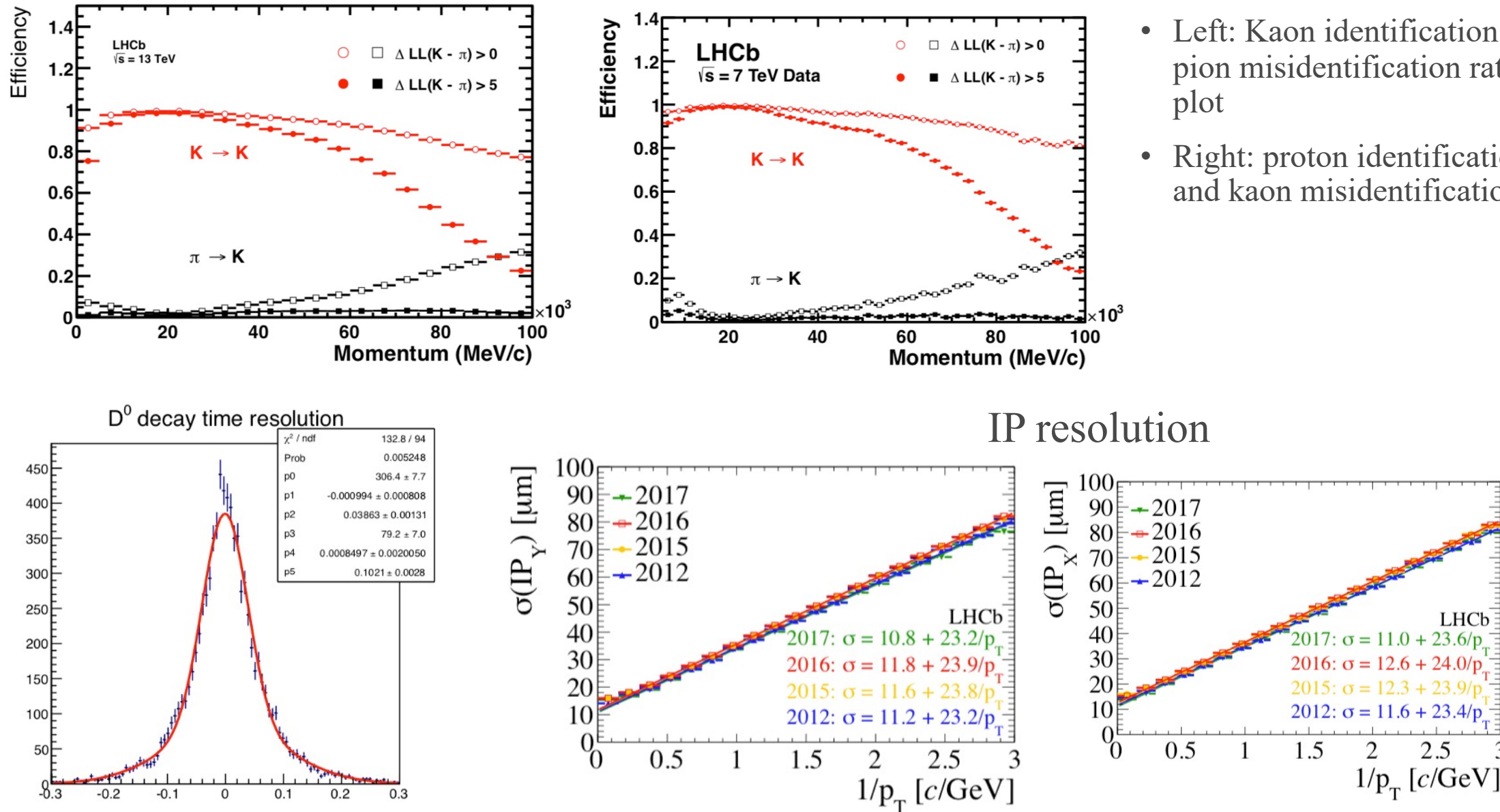


Thank you for your
attention

Back Up

LHCb performances

41



- Left: Kaon identification efficiency and pion misidentification rate Right: same plot
- Right: proton identification efficiency and kaon misidentification fraction.

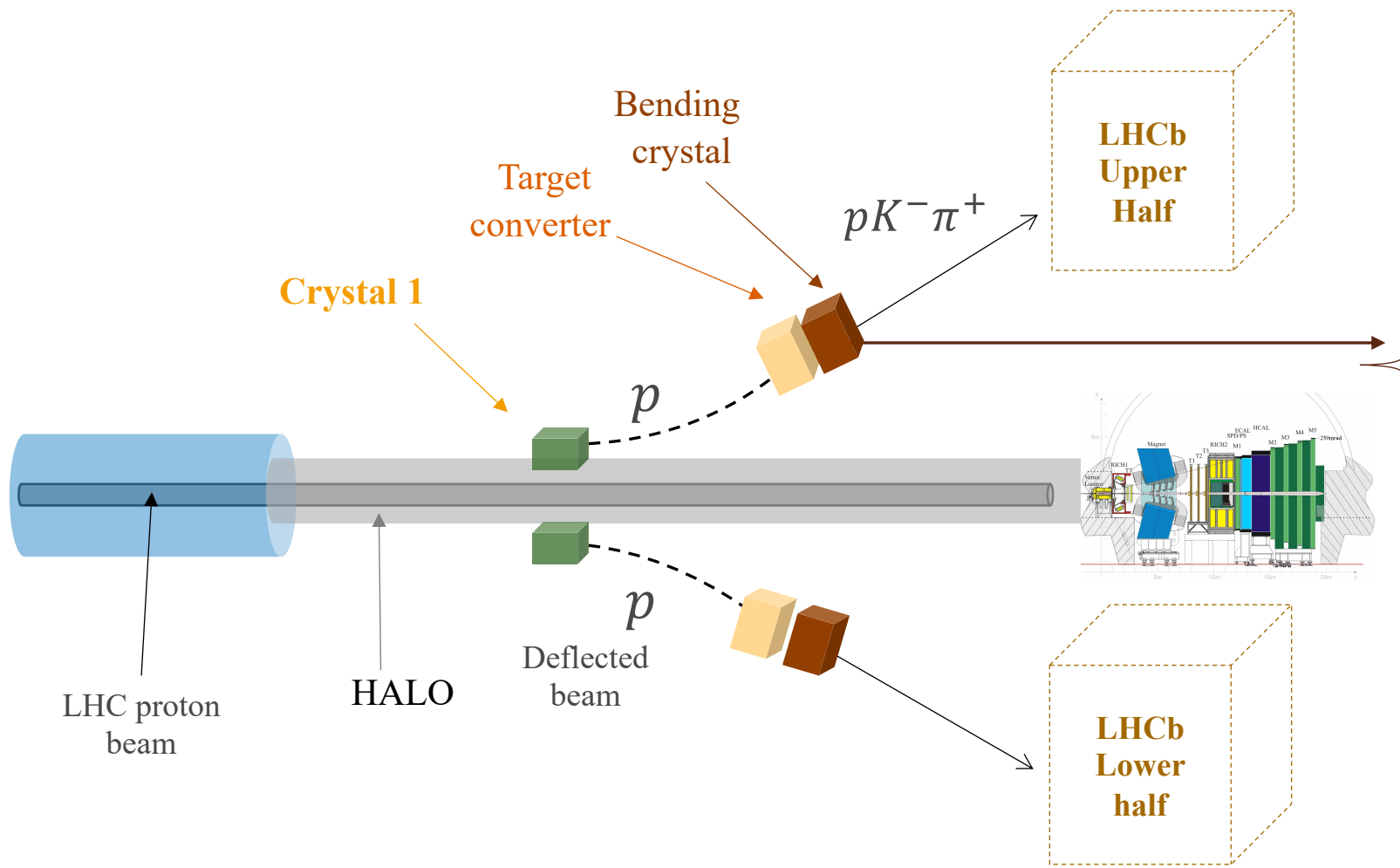
IP resolution

MDM measurement

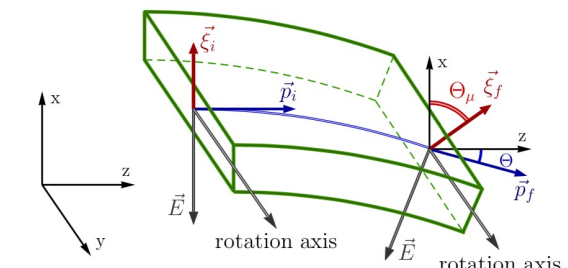
Bending crystal experiment

43

Proposal for double crystal setup at LHCb



$$\Theta_\mu \approx \gamma \left(\frac{g}{2} - 1 \right) \Theta$$



Need initial ($\vec{\xi}_i$) and final ($\vec{\xi}_f$) Λ_c^+ polarization

$\vec{\xi}_i$: Produce polarized baryons using a target-crystal before the bending crystal

$\vec{\xi}_f$: Measured using dedicated experiment or LHCb

Magnetic dipole moments (MDM): baryons

44

Baryons MDM:

- proton and neutron measured.
- short lived → need for a new technique

$c\tau$	Comments	$g - \text{factor} - \text{exp.}$
p	Quark model description	+ 5.585 694 702 (17) ^a
n	$\mu_n = -\frac{2}{3}\mu_p$ satisfied	- 3.826 085 45 (90) ^b
Σ^+	2.4 cm Measured using bent crystals	+ 6.1 ±(12) _{stat} ±(10) _{sys}
Λ_c^+	60 μm Not measured	--

Decay asymmetry parameters for Λ_c^+ decays

45

PDG average

▼ Λ_c^+ DECAY PARAMETERS

α FOR $\Lambda_c^+ \rightarrow \Lambda\pi^+$ -0.84 ± 0.09

α FOR $\Lambda_c^+ \rightarrow \Sigma^+\pi^0$ -0.55 ± 0.11

α FOR $\Lambda_c^+ \rightarrow \Sigma^0\pi^+$ -0.73 ± 0.18

α FOR $\Lambda_c^+ \rightarrow \Lambda\ell^+\nu_\ell$ -0.86 ± 0.04

α FOR $\Lambda_c^+ \rightarrow pK_S^0$ 0.2 ± 0.5

Theory predictions

TABLE I: Branching fractions (upper entry) and up-down decay asymmetries α (lower entry) of Cabibbo-allowed $\Lambda_c^+ \rightarrow \mathcal{B} + P$ decays in various models. Model results of [8–10, 12] have been normalized using the current world average of $\tau(\Lambda_c^+)$ [7]. Branching fractions cited from [13] are for $\phi_{\eta-\eta'} = -23^\circ$ and $r \equiv |\psi^{\mathcal{B}_c}(0)|^2/|\psi^{\mathcal{B}}(0)|^2 = 1.4$.

Decay	Körner, Krämer [8]	Xu, Kamal [9]	Cheng, Tseng [10] CA Pole	Ivanov et al [11]	Żenczykowski [12]	Sharma, Verma [13]	Expt. [7]
$\Lambda_c^+ \rightarrow \Lambda\pi^+$	input	1.62	1.46 0.88	0.79	0.52	1.12	1.30 ± 0.07
$\Lambda_c^+ \rightarrow p\bar{K}^0$	input	1.20	3.64 1.26	2.06	1.71	1.64	3.16 ± 0.16
$\Lambda_c^+ \rightarrow \Sigma^0\pi^+$	0.32	0.34	1.76 0.72	0.88	0.39	1.34	1.29 ± 0.07
$\Lambda_c^+ \rightarrow \Sigma^+\pi^0$	0.32	0.34	1.76 0.72	0.88	0.39	1.34	1.24 ± 0.10
$\Lambda_c^+ \rightarrow \Sigma^+\eta$	0.16			0.11	0.90	0.57	0.70 ± 0.23
$\Lambda_c^+ \rightarrow \Sigma^+\eta'$	1.28			0.12	0.11	0.10	
$\Lambda_c^+ \rightarrow \Xi^0K^+$	0.26	0.10		0.31	0.34	0.13	0.50 ± 0.12
$\Lambda_c^+ \rightarrow \Lambda\pi^+$	-0.70	-0.67	-0.99 -0.95	-0.95	-0.99	-0.99	-0.91 ± 0.15
$\Lambda_c^+ \rightarrow p\bar{K}^0$	-1.0	0.51	-0.90 -0.49	-0.97	-0.66	-0.99	
$\Lambda_c^+ \rightarrow \Sigma^0\pi^+$	0.70	0.92	-0.49 0.78	0.43	0.39	-0.31	
$\Lambda_c^+ \rightarrow \Sigma^+\pi^0$	0.70	0.92	-0.49 0.78	0.43	0.39	-0.31	-0.45 ± 0.32
$\Lambda_c^+ \rightarrow \Sigma^+\eta$	0.33			0.55	0	-0.91	
$\Lambda_c^+ \rightarrow \Sigma^+\eta'$	-0.45			-0.05	-0.91	0.78	
$\Lambda_c^+ \rightarrow \Xi^0K^+$	0	0		0	0	0	

P.A. Zyla *et al.* (Particle Data Group),
 Prog. Theor. Exp. Phys. 2020, 083C01 (2020) and 2021 update.

PDG 2020 Λ_c^+ decays

▼ Hadronic modes with a p or n : $S = -1$ final states

Γ_1	pK_S^0	$(1.59 \pm 0.08)\%$
Γ_2	$pK^-\pi^+$	$(6.28 \pm 0.32)\%$
Γ_3	$p\bar{K}^*(892)^0$	$(1.96 \pm 0.27)\%$
Γ_4	$\Delta(1232)^{++}K^-$	$(1.08 \pm 0.25)\%$
Γ_5	$\Lambda(1520)\pi^+$	$(2.2 \pm 0.5)\%$
Γ_6	$pK^-\pi^+$ nonresonant	$(3.5 \pm 0.4)\%$
Γ_7	$pK_S^0\pi^0$	$(1.97 \pm 0.13)\%$
Γ_8	$nK_S^0\pi^+$	$(1.82 \pm 0.25)\%$
Γ_9	$p\bar{K}^0\eta$	$(1.6 \pm 0.4)\%$
Γ_{10}	$pK_S^0\pi^+\pi^-$	$(1.60 \pm 0.12)\%$
Γ_{11}	$pK^-\pi^+\pi^0$	$(4.46 \pm 0.30)\%$
Γ_{12}	$pK^*(892)^-\pi^+$	$(1.4 \pm 0.5)\%$
Γ_{13}	$p(K^-\pi^+)$ nonresonant π^0	$(4.6 \pm 0.8)\%$
Γ_{14}	$\Delta(1232)\bar{K}^*(892)$	seen
Γ_{15}	$pK^-2\pi^+\pi^-$	$(1.4 \pm 0.9) \times 10^{-3}$
Γ_{16}	$pK^-\pi^+2\pi^0$	$(1.0 \pm 0.5)\%$

▼ Hadronic modes with a hyperon: $S = -1$ final states

Γ_{28}	$\Lambda\pi^+$	$(1.30 \pm 0.07)\%$	$S=1.1$	864	▼
Γ_{29}	$\Lambda\pi^+\pi^0$	$(7.1 \pm 0.4)\%$	$S=1.1$	844	▼
Γ_{30}	$\Lambda\rho^+$	$< 6\%$	$CL=95\%$	636	▼
Γ_{31}	$\Lambda\pi^-2\pi^+$	$(3.64 \pm 0.29)\%$	$S=1.4$	807	▼
Γ_{32}	$\Sigma(1385)^+\pi^+\pi^-$, $\Sigma^{*+} \rightarrow \Lambda\pi^+$	$(1.0 \pm 0.5)\%$		688	▼
Γ_{33}	$\Sigma(1385)^-2\pi^+$, $\Sigma^{*-} \rightarrow \Lambda\pi^-$	$(7.6 \pm 1.4) \times 10^{-3}$		688	▼
Γ_{34}	$\Lambda\pi^+\rho^0$	$(1.5 \pm 0.6)\%$		524	▼
Γ_{35}	$\Sigma(1385)^+\rho^0$, $\Sigma^{*+} \rightarrow \Lambda\pi^+$	$(5 \pm 4) \times 10^{-3}$		363	▼
Γ_{36}	$\Lambda\pi^-2\pi^+$ nonresonant	$< 1.1\%$	$CL=90\%$	807	▼
Γ_{37}	$\Lambda\pi^-\pi^02\pi^+$ total	$(2.3 \pm 0.8)\%$		757	▼
Γ_{38}	$\Lambda\pi^+\eta$	$(1.84 \pm 0.26)\%$		691	▼
Γ_{39}	$\Sigma(1385)^+\eta$	$(9.1 \pm 2.0) \times 10^{-3}$		570	▼
Γ_{40}	$\Lambda\pi^+\omega$	$(1.5 \pm 0.5)\%$		517	▼
Γ_{41}	$\Lambda\pi^-\pi^02\pi^+$, no η or ω	$< 8 \times 10^{-3}$	$CL=90\%$	757	▼
Γ_{42}	$\Lambda K^+\bar{K}^0$	$(5.7 \pm 1.1) \times 10^{-3}$	$S=1.9$	443	▼
Γ_{43}	$\Xi(1690)^0K^+$, $\Xi^{*0} \rightarrow \Lambda\bar{K}^0$	$(1.6 \pm 0.5) \times 10^{-3}$		286	▼
Γ_{44}	$\Sigma^0\pi^+$	$(1.29 \pm 0.07)\%$	$S=1.1$	825	▼
Γ_{45}	$\Sigma^+\pi^0$	$(1.25 \pm 0.10)\%$		827	▼
Γ_{46}	$\Sigma^+\eta$	$(4.4 \pm 2.0) \times 10^{-3}$		713	▼
Γ_{47}	$\Sigma^+\eta'$	$(1.5 \pm 0.6)\%$		391	▼
Γ_{48}	$\Sigma^+\pi^+\pi^-$	$(4.50 \pm 0.25)\%$	$S=1.3$	804	▼

Magnetic dipole moments (MDM): Λ_c^+

47

Prediction for Λ_c^+ MDM: suffers from uncertainty on the charm quark mass: $m_c = 1.27 \pm 0.02$ GeV

- Quark model

$$\mu_{\Lambda_c^+} = \langle \Lambda_c^+; \frac{1}{2}, +\frac{1}{2} | (\vec{\mu}_1 + \vec{\mu}_2 + \vec{\mu}_3) \cdot \vec{S}_z | \Lambda_c^+; \frac{1}{2}, +\frac{1}{2} \rangle \quad \rightarrow \quad \boxed{\mu_{\Lambda_c^+} = \mu_c}$$

- Inserting the constituent quark mass:

$$\mu_{\Lambda_c^+} = 0.37 \frac{g_c}{2} \mu_N \qquad \mu_N = \frac{e \hbar}{2m_p}$$

- All predictions: $[0.15 - 0.52]\mu_N$
- Prediction using: radiative charmonium decays: using BES III experimental data without any charm quark mass uncertainty

[Eur.Phys.J.C 80 \(2020\) 5, 358](#)

$$\frac{g_c}{2m_c} = 0.76 \pm 0.05 \text{ GeV}^{-1}$$

Experimental input

$$\mu_{\Lambda_c} = \mu_c = \frac{g_c}{2m_c} \frac{2}{3} m_p \mu_N = (0.48 \pm 0.03) \mu_N$$

Prediction

MDM Λ_c^+ predictions

48

- Prediction for Λ_c^+ MDM

nb.	$\mu_{\Lambda_c^+} [\mu_N]$	Approach
1	0.15 ± 0.05	QCD spectral sum rule
2	0.24 ± 0.02	NNLO in the HHCPT
5	$0.33 - 0.34$	Interquark potential and Fadeev formalism
3	0.34	Independent quark model, power-law potential
4	$0.369 - 0.385$	Hyper central Coulomb plus power potential
5	$0.36 - 0.41$	5q components contributions
6	0.37	Chiral perturbation theory
7	0.38	Soliton model and chiral perturbation theory
8	0.392	SU(4) chiral constituent quark model
9	0.40 ± 0.05	Light cone QCD sum rules
10	0.411	Bag model reexamined
11	0.42 ± 0.01	Relativistic three-quark model
12	0.48 ± 0.03	Radiative charmonium decays
13	0.52	Dirac point-form dynamics

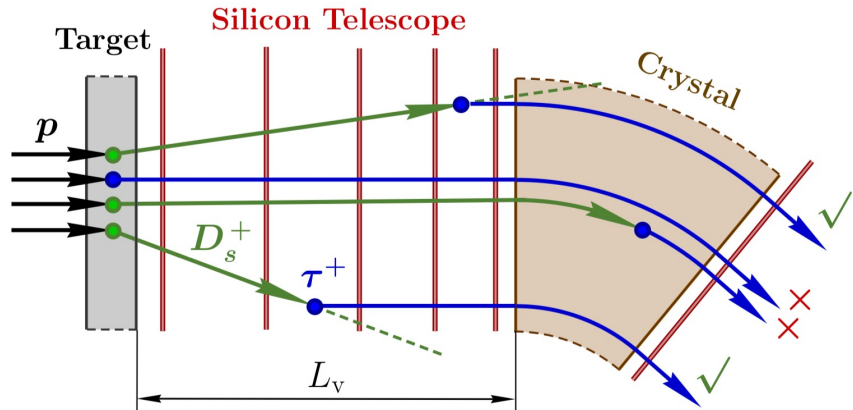
τ MDM measurement

49

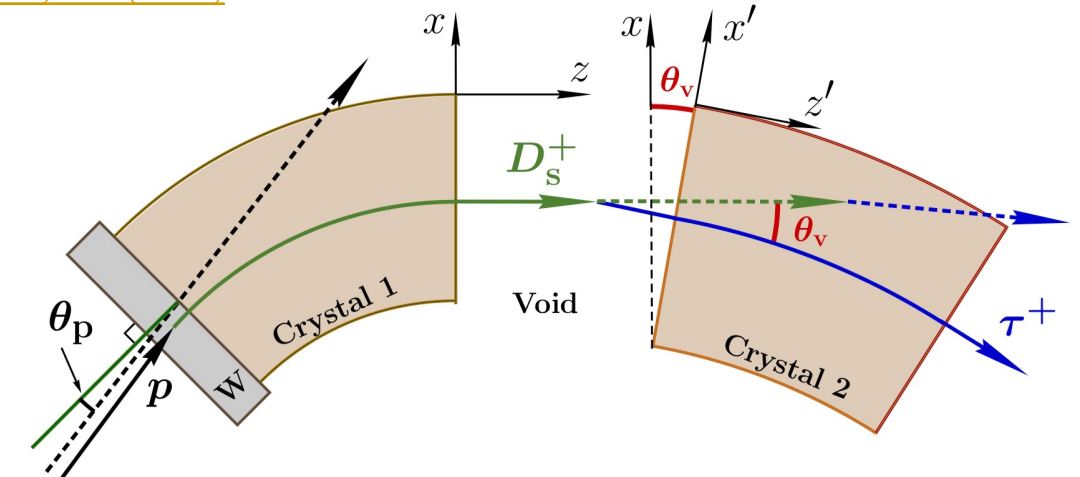
- SM prediction: $a_\tau = 0.0017721(5) \rightarrow g_\tau = 2.0035442(8)$ [Eur.Phys.J.C 35 \(2004\) 159-170](#)
- Measurement: $-0.052 < a_\tau < +0.013$. Measured by DELPHI, process: $e^+e^- \rightarrow e^+e^-\tau^+\tau^-$
- $\gamma\tau\tau$ vertices : MDM is extracted by comparing the measured cross-section with QED expectations
- Other methods proposed : $\tau^- \rightarrow l^-\nu_\tau \bar{\nu}_l \gamma$ at Super-KEKB [JHEP 03 \(2016\) 140](#)

Use bent crystals: $p p \rightarrow D_s^+ X, \quad D_s^+ \rightarrow \tau^+ \nu_\tau, \quad \tau^+$ flight in the crystal, $\tau^+ \rightarrow \pi^+ \pi^+ \pi^- \bar{\nu}_\tau$.

[J. High Energ. Phys. 2019, 156 \(2019\)](#)



Remove $X \rightarrow 2\pi^+\pi^-$ background (need accurate measurement of D_s^+ and τ^+ momenta)

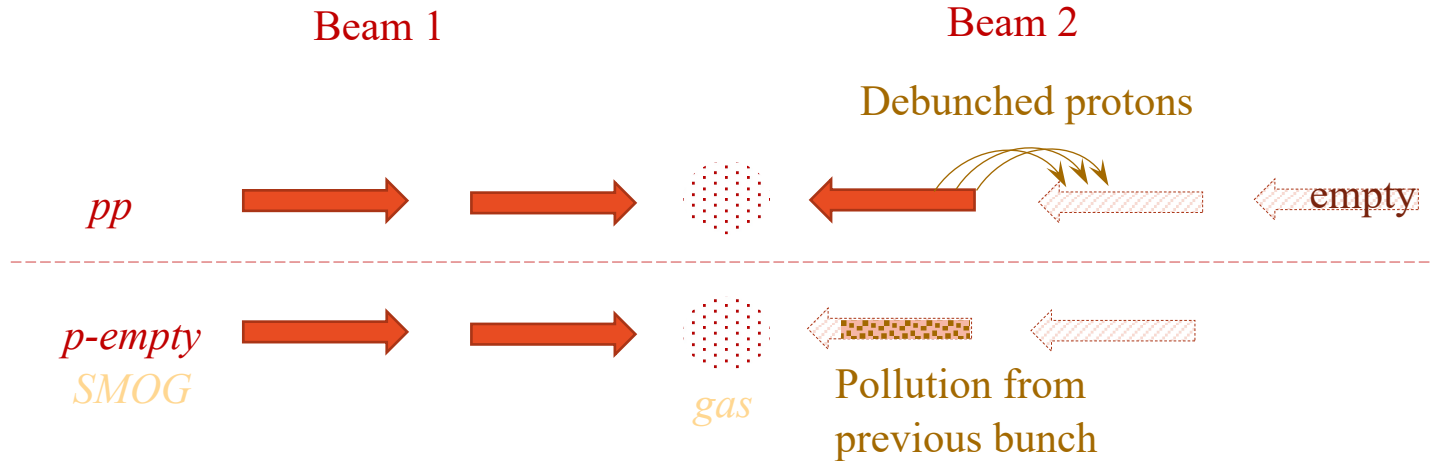
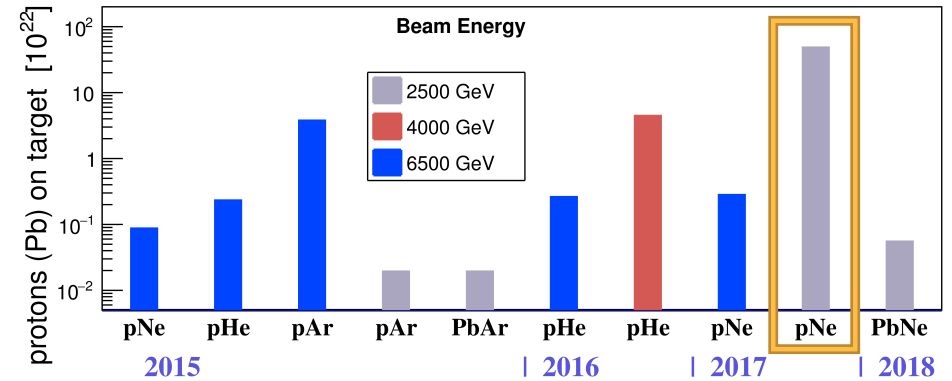


1 crystal for channeling D_s^+ mesons \rightarrow constrain momentum
2nd crystal to precess the τ leptons

SMOG pollution

50

- Data sample: 2.5 TeV protons on Neon, center of mass energy of 68.9 GeV
- Data are taken simultaneously with pp collisions at 5 TeV, no special runs.
- Major problem: pollution from pp collisions « ghost charges ».
 - ❖ pp and p-Gas data are taken at the same time alternating full and empty bunches.
 - ❖ Some debunched protons from the previous beam go to the following bunch which is supposed to be empty.

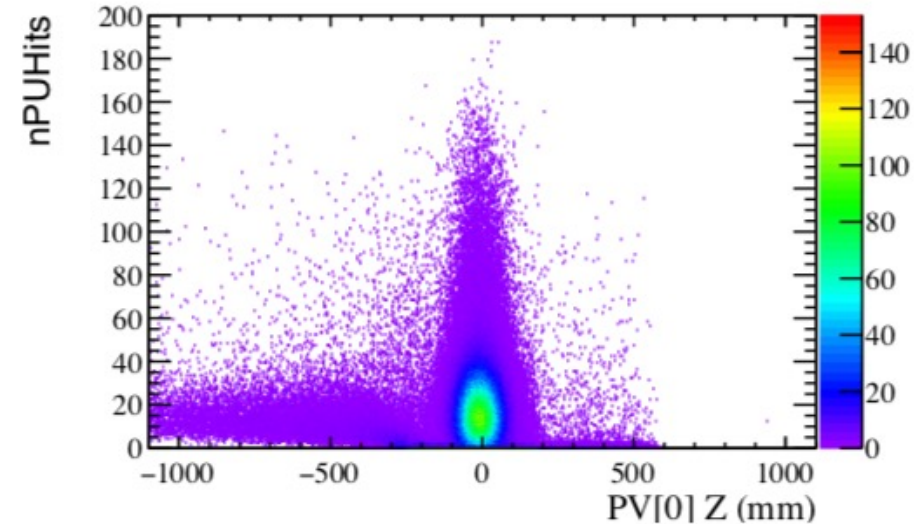
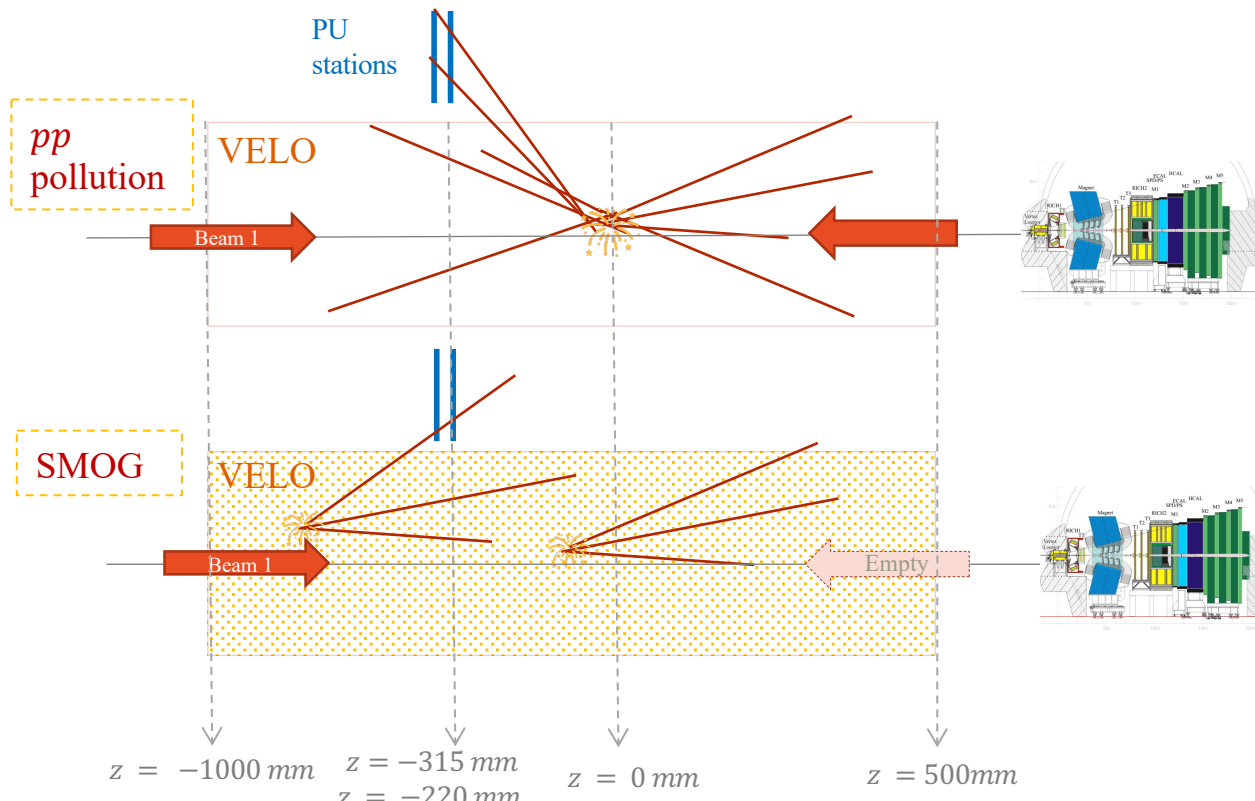


SMOG pollution

51

Cleaning using the event topology:

- Z coordinate of the PV: SMOG has a larger PVZ region
- Number of hits in the Pile Up stations of VELO at $z = -315$ and $z = -220$ mm → small for SMOG events which are forward
- Number of reconstructed tracks (nTracks) pointing opposite to the LHC



	$-200 < Z_{PV} < -100$	$-100 < Z_{PV} < +100$	$+100 < Z_{PV} < +200$
nPUHits=0 - GC	$(0.64 \pm 0.31)\%$	$(8.93 \pm 3.27)\%$	$(0.57 \pm 0.34)\%$
nPUHits=0 - SL	$(24.32 \pm 1.16)\%$	$(31.26 \pm 0.88)\%$	$(21.35 \pm 1.28)\%$
Correction factor	1.235 ± 0.012	1.195 ± 0.044	1.207 ± 0.013
nPUHits<3 - GC	$(2.25 \pm 0.47)\%$	$(29.44 \pm 4.77)\%$	$(1.84 \pm 0.56)\%$
nPUHits<3 - SL	$(14.86 \pm 0.91)\%$	$(24.32 \pm 0.77)\%$	$(14.23 \pm 1.04)\%$
correction factor	1.123 ± 0.010	0.877 ± 0.060	1.121 ± 0.012
nPUHits<5 - GC	$(4.69 \pm 0.62)\%$	$(49.08 \pm 5.35)\%$	$(3.76 \pm 0.78)\%$
nPUHits<5 - SL	$(11.91 \pm 0.81)\%$	$(21.79 \pm 0.73)\%$	$(12.17 \pm 0.96)\%$
correction factor	1.067 ± 0.010	0.620 ± 0.065	1.080 ± 0.013

Table 7: GC: Fraction of Ghost-Charge residual contamination after **nPUHits** cut; SL: fraction of fixed-target Signal Loss after **nPUHits** cut. Correction factor is given by $(1 - GC) \times (1 + SL)$

Global event cuts for 2017 pNe SMOG data. Technical report, CERN, Geneva, Jun 2020. <https://cds.cern.ch/record/2720461>.

Formalism

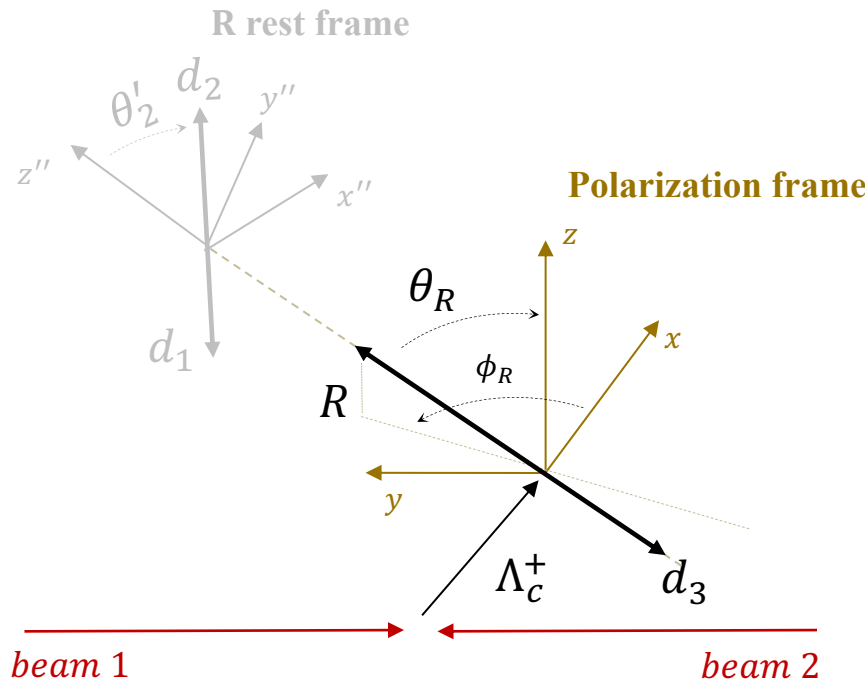
Helicity formalism

53

Helicity operator: invariance under rotations and boosts along \hat{p}

$$\Lambda = \frac{\vec{J} \cdot \vec{p}}{\|\vec{p}\|} = (\vec{L} + \vec{S}) \cdot \hat{\mathbf{p}} = \vec{S} \cdot \hat{\mathbf{p}}$$

The helicity frame: frame where the particle momentum is aligned to the z-axis and the particle is at rest.
In this frame the spin projection $s_z \equiv \lambda$

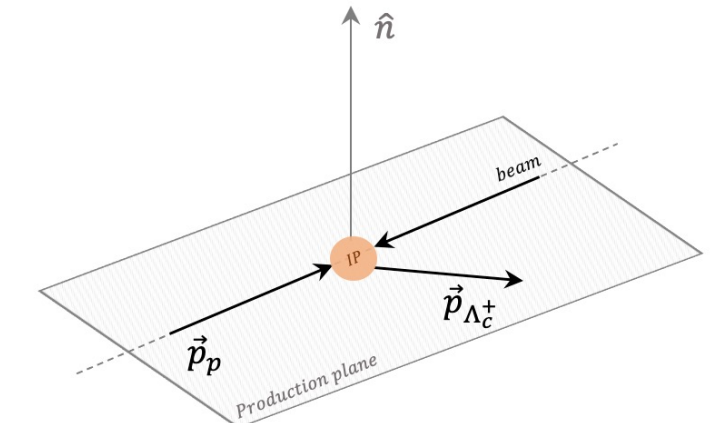


Polarization frame: polarization expected *perpendicular to the production plane* due to parity conservation in strong interactions.

$$z = \hat{p}_{beam} \times \hat{p}_{\Lambda_c^+}^{lab}$$

$$y = -\hat{p}_{beam}$$

$$x = \hat{p}_{\Lambda_c^+}^{lab}$$



From single chain to the total amplitude

54

Amplitude for each chain: **lineshape** \times rotations

parametrized by D -Wigner functions:
 $D_{m,\lambda}^J(\theta, \varphi, 0)$

1. One rotation to align the resonance helicity frame
2. One rotation to align proton helicity frame
3. Helicity couplings

	J^P
Λ_c^+	$\frac{1}{2}^-$
p	$\frac{1}{2}^-$
K	0^-
π^+	0^-

Lineshape



$$\Lambda_c^+ \rightarrow (K^* \rightarrow K^- \pi^+) p$$

$$A_{K^*}(m, \lambda_p) = B_{K^*}(m_{K\pi}) \sum_{s_{K^*}} \sum_{\lambda_{K^*}} D_{\lambda_{K^*}, 0}^{s_{K^*}}(\phi'_K, \theta'_K, 0) D_{m, \lambda_{K^*} - \lambda_p}^{\frac{1}{2}^*}(\phi_{K^*}, \theta_{K^*}, 0) b_{\lambda_p} a_{\lambda_{K^*}}$$

From single chain to the total amplitude

55

Amplitude for each chain: **lineshape** \times **rotations**

parametrized by D -Wigner functions:
 $D_{m,\lambda}^J(\theta, \varphi, 0)$

1. One rotation to align the resonance helicity frame
2. One rotation to align proton helicity frame
3. Helicity couplings

	J^P
Λ_c^+	$\frac{1}{2}^-$
p	$\frac{1}{2}^-$
K	0^-
π^+	0^-

$$\Lambda_c^+ \rightarrow (K^* \rightarrow K^- \pi^+) p \quad A_{K^*}(m, \lambda_p) = B_{K^*}(m_{K\pi}) \sum_{s_{K^*}} \sum_{\lambda_{K^*}} D_{\lambda_{K^*}, 0}^{s_{K^*}*}(\phi'_K, \theta'_K, 0) D_{m, \lambda_{K^*} - \lambda_p}^{\frac{1}{2}*}(\phi_{K^*}, \theta_{K^*}, 0) b_{\lambda_p} a_{\lambda_{K^*}}$$

From single chain to the total amplitude

56

Amplitude for each chain: **lineshape** \times **rotations**

parametrized by D -Wigner functions:
 $D_{m,\lambda}^J(\theta, \varphi, 0)$

1. One rotation to align the resonance helicity frame
2. One rotation to align proton helicity frame
3. Helicity couplings

	J^P
Λ_c^+	$\frac{1}{2}^-$
p	$\frac{1}{2}^-$
K	0^-
π^+	0^-

$$\Lambda_c^+ \rightarrow (K^* \rightarrow K^- \pi^+) p \quad A_{K^*}(m, \lambda_p) = B_{K^*}(m_{K\pi}) \sum_{s_{K^*}} \sum_{\lambda_{K^*}} D_{\lambda_{K^*}, 0}^{s_{K^*}}(\phi'_{K^*}, \theta'_{K^*}, 0) D_{m, \lambda_{K^*} - \lambda_p}^{\frac{1}{2}^*}(\phi_{K^*}, \theta_{K^*}, 0) b_{\lambda_p} a_{\lambda_{K^*}}$$

From single chain to the total amplitude

57

Amplitude for each chain: **lineshape** \times **rotations**

parametrized by D -Wigner functions:
 $D_{m,\lambda}^J(\theta, \varphi, 0)$

1. One rotation to align the resonance helicity frame
2. One rotation to align proton helicity frame
3. Helicity couplings

	J^P
Λ_c^+	$\frac{1}{2}^-$
p	$\frac{1}{2}^-$
K	0^-
π^+	0^-

$$\Lambda_c^+ \rightarrow (K^* \rightarrow K^- \pi^+) p \quad A_{K^*}(m, \lambda_p) = B_{K^*}(m_{K\pi}) \sum_{s_{K^*}} \sum_{\lambda_{K^*}} D_{\lambda_{K^*}, 0}^{s_{K^*}*}(\phi'_K, \theta'_K, 0) D_{m, \lambda_{K^*} - \lambda_p}^{\frac{1}{2}*}(\phi_{K^*}, \theta_{K^*}, 0) b_{\lambda_p} a_{\lambda_{K^*}}$$

$$\Lambda_c^+ \rightarrow (\Delta^{++} \rightarrow p \pi^+) K^- \quad A_{\Delta}(m, \lambda_p) = B_{\Delta}(m_{p\pi}) \sum_{s_{\Delta}} \sum_{\lambda_{\Delta}} D_{\lambda_{\Delta}, -\lambda_p}^{s_{\Delta}*}(\phi'_{\pi}, \theta'_{\pi}, 0) D_{m, \lambda_{\Delta}}^{\frac{1}{2}*}(\phi_{\Delta}, \theta_{\Delta}, 0) d_{\lambda_p} c_{\lambda_{\Delta}}$$

$$\Lambda_c^+ \rightarrow (\Lambda^* \rightarrow p K^-) \pi^+ \quad A_{\Lambda^*}(m, \lambda_p) = B_{\Lambda^*}(m_{pK}) \sum_{s_{\Lambda^*}} \sum_{\lambda_{\Lambda^*}} D_{\lambda_{\Lambda^*}, \lambda_p}^{s_{\Lambda^*}*}(\phi_p, \theta_p, 0) D_{m, \lambda_{\Lambda^*}}^{\frac{1}{2}*}(\phi_{\Lambda^*}, \theta_{\Lambda^*}, 0) f_{\lambda_p} e_{\lambda_{\Lambda^*}}$$

Sum over
the isobars

Parity conservation

58

- If parity is conserved, Lagrangian must be invariant
- The terms containing spin and momenta must be invariant
→ the odd terms must have zero expectation value
- Λ_c^+ production, vectors available: \vec{p}_p proton momentum, $\vec{p}_{\Lambda_c^+}$ baryon direction and $\vec{P}_{\Lambda_c^+}$ polarization vector.
- Scalar term available which is parity conserving: $\vec{P}_{\Lambda_c^+}(\vec{p}_p \times \vec{p}_{\Lambda_c^+})$

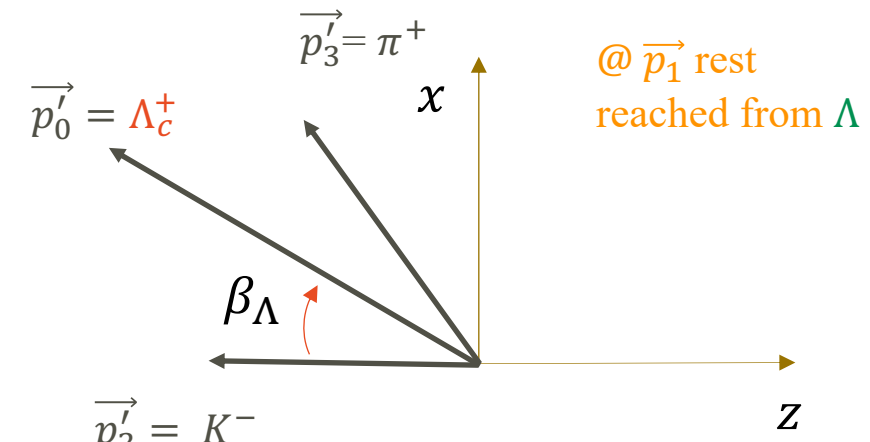
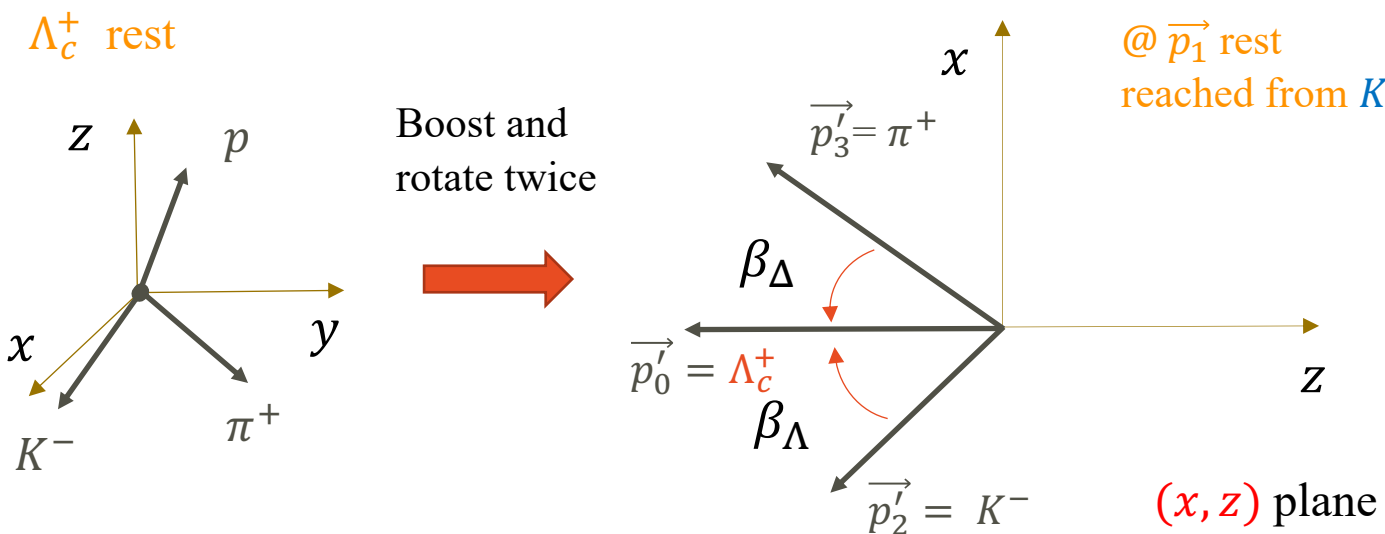
$$\mathcal{A}(\vec{p}_i, \vec{S}_i) = \mathcal{A}(-\vec{p}_i, \vec{S}_i)$$

Marco Sozzi. Discrete symmetries and CP violation: from experiment to theory.

Obs.	P	C	T
Time (t)	t	t	$-t$
Position (\vec{r})	$-\vec{r}$	\vec{r}	\vec{r}
Energy (E)	E	E	E
Momentum (\vec{p})	$-\vec{p}$	\vec{p}	$-\vec{p}$
Angular momentum (\vec{J})	\vec{J}	\vec{J}	$-\vec{J}$
Helicity (λ)	$-\lambda$	λ	λ
Electric charge (e)	e	$-e$	e

Helicity formalism : Wigner rotation, polar part

59



Boost along z direction:

$$\begin{aligned} t' &= \gamma \left(t - \frac{v}{c^2} z \right) \\ x' &= x \\ y' &= y \\ z' &= \gamma(z - vt) \end{aligned}$$

K^* chain :

$$\Lambda_c^+ \rightarrow (K^* \rightarrow K^- \pi^+) p$$

boost from $\vec{p}_{\Lambda_c^+} = 0$ along $\vec{p}_1 \parallel z \rightarrow$
 $\vec{p}'_{\Lambda_c^+} \parallel -z$

Need to rotate
around y axis of
beta angles

Λ^* chain :

$$\Lambda_c^+ \rightarrow (\Lambda^* \rightarrow p K^-) \pi^+$$

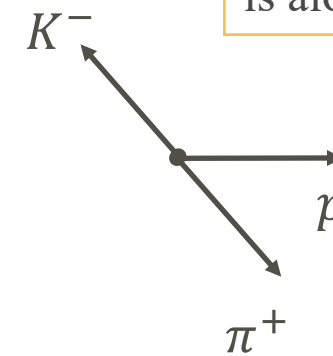
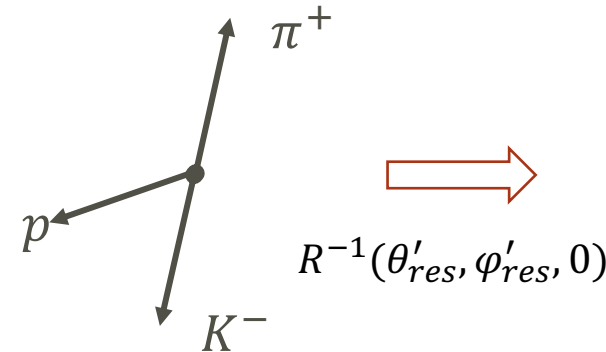
boost from \vec{p}_0 along $\Lambda^* \rightarrow \vec{p}'_2 \parallel -z$

Helicity formalism : Wigner rotation, azimuthal part 60

Need also an extra phase for the K^* channel

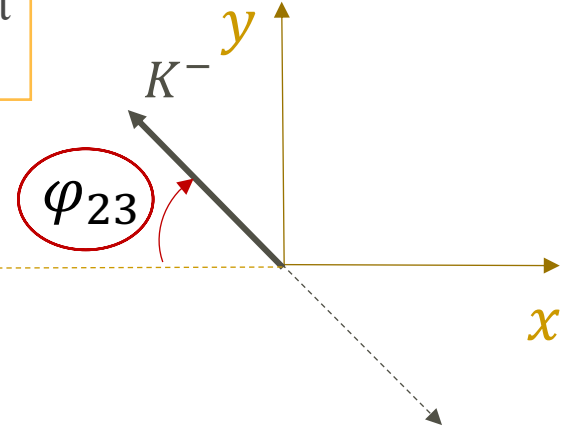
$\text{@ } K^* \text{ rest}$

$$\Lambda_c^+ \rightarrow (K^* \rightarrow K^- \pi^+) p$$

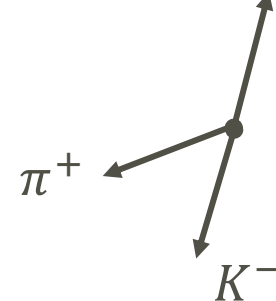


Boost to p rest frame:
x,y component don't
change since the boost
is along z

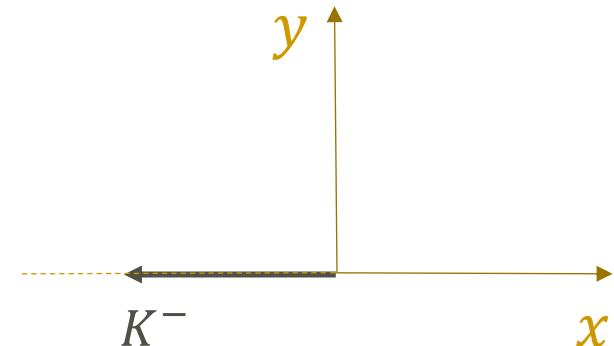
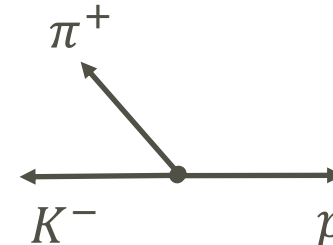
(y, x) plane



$$\Lambda_c^+ \rightarrow (\Lambda^* \rightarrow p K^-) \pi^+ \text{ @ } \Lambda^* \text{ rest}$$



$$R^{-1}(\theta'_{res}, \varphi'_{res}, 0)$$



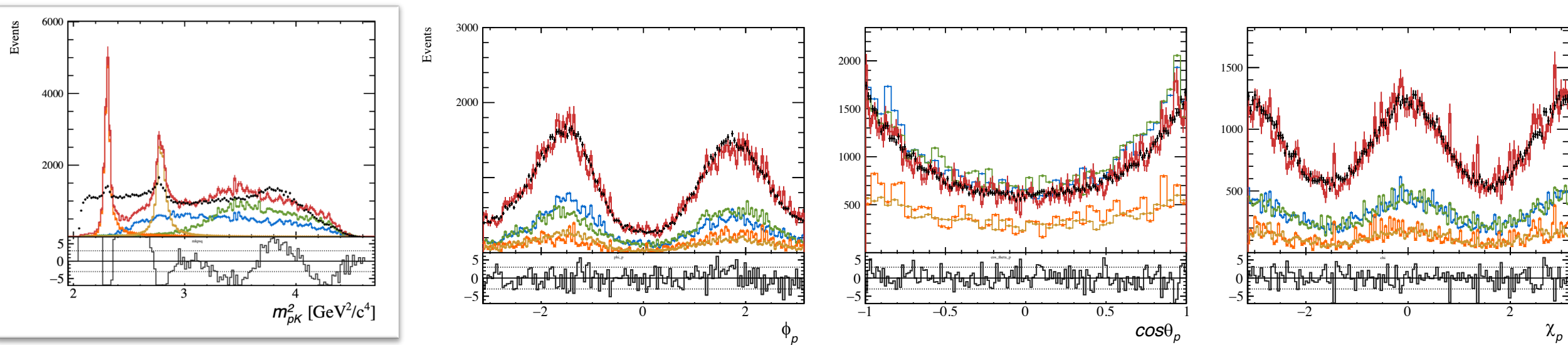
Analysis

Model choice

62

- List of known resonances large, all possibly contributing
- Model building: assess which resonances contributes to the fit. Strategy:
 1. Add resonances which are visible by eye
 2. **Model building**, add resonances **iteratively**:
 - Fix polarization to zero → angles have no influence

Example: Minimal model, very bad fit for m_{pK^-} mass, however angles are well described



Other offline selections

63

Tighten HLT2 selections: handmade optimization is enough thanks to high statistics

Three main categories:

1. Λ_c^+ selections:

- Prompt separation
- Reasonable lifetime
- Good vertex quality
- Good momentum reconstruction (DIRA)

2. p/p_T selections: better PID performances

3. PID: reduce the misidentification probability

Particle	Selections
Λ_c^+	$\log(\chi_{\text{IP}}^2) < -2.$ $\tau < 0.0015 \text{ ns}$ $\chi_{FD}^2 > 40$ $\chi_{\text{vtx}}^2/\text{ndf} < 5$ $\text{acos}(DIRA) > 10 \text{ mrad}$
Proton	$\chi_{\text{IP}}^2 > 9$ $\chi_{\text{IP}}^2 < 200$ $p_{\text{ghost}}(p) < 0.4$ $10000 < p < 100000 \text{ MeV}/c$ $p_T > 1000 \text{ MeV}/c$
Kaon	$\chi_{\text{IP}}^2 > 9$ $\chi_{\text{IP}}^2 < 200$ $3000 < p < 150000 \text{ MeV}/c$ $p_T > 500 \text{ MeV}/c$
Pion	$\chi_{\text{IP}}^2 > 9$ $\chi_{\text{IP}}^2 < 200$ $3000 < p < 150000 \text{ MeV}/c$ $p_T > 500 \text{ MeV}/c$
PID (MC15TuneV1)	$(\text{ProbNN}_p(p) - \text{ProbNN}_K(p)) > 0.1$ $(\text{ProbNN}_p(p) - p \text{ProbNN}_\pi(p)) > 0.4$ $\text{ProbNN}_K(K) > 0.1$

Resonances : Λ^*

Resonance	Mass (approx)[MeV]	Width (approx)[MeV]	J^P	$L_{\Lambda_c^+}$	L_R	PDG status
<i>pK channel</i>						
$\Lambda^*(1405)$	$1405.1^{+1.3}_{-1.0}$	50.5 ± 2.0	$1/2^-$	0,1	0	****
$\Lambda^*(1520)$	1517 ± 4	15^{+10}_{-8}	$3/2^-$	1,2	2	****
$\Lambda^*(1600)$	1544 ± 3	112^{+12}_{-2}	$1/2^+$	0,1	1	***
$\Lambda^*(1670)$	1669^{+3}_{-8}	19^{+18}_{-2}	$1/2^-$	0,1	0	****
$\Lambda^*(1690)$	1697 ± 6	65 ± 14	$3/2^-$	1,2	2	****
$\Lambda^*(1800)$	1720-1850	200-400	$1/2^-$	0,1	0	***
$\Lambda^*(1810)$	1750-1850	50-250	$1/2^+$	0,1	1	***
$\Lambda^*(1820)$	1824^{+2}_{-1}	77 ± 2	$5/2^+$	2,3	3	****
$\Lambda^*(1830)$	1899 ± 40	80^{+100}_{-34}	$5/2^-$	2,3	2	****
$\Lambda^*(1890)$	1850-1910	60-200	$3/2^+$	1,2	1	****
$\Lambda^*(2000)$	2000	0.150	-	-	-	*
$\Lambda^*(2100)$	2090-2110	100-250	$7/2^-$	3,4	4	****
$\Lambda^*(2110)$	2090-2140	150-250	$5/2^+$	2,3	3	***
$\Sigma^*(1660)$	$1660 \in [1640 - 1680]$	$220 \in [100 - 300]$	$1/2^+$	0,1	1	***
$\Sigma^*(1670)$	$1675 \in [1665 - 1685]$	$70 \in [40 - 100]$	$3/2^-$	1,2	2	****
$\Sigma^*(1750)$	$1750 \in [1700 - 1800]$	$150 \in [100 - 200]$	$1/2^-$	0,1	0	***
$\Sigma^*(1775)$	$1775 \in [1770 - 1780]$	$120 \in [105 - 135]$	$5/2^-$	2,3	2	****
$\Sigma^*(1910)$	$1910 \in [1870 - 1950]$	$220 \in [150 - 300]$	$3/2^-$	1,2	2	****
$\Sigma^*(1915)$	$1915 \in [1900 - 1935]$	$120 \in [80 - 160]$	$5/2^+$	2,3	3	****
$\Sigma^*(2030)$	$2030 \in [2015 - 2040]$	$180 \in [150 - 200]$	$7/2^+$	3,4	3	****

Resonances : Δ^{++} and K^*

65

$p\pi$ channel

$\Delta^{++}(1232)$	1209-1211	98-102	$3/2^+$	1,2	1	****
$\Delta^{++}(1600)$	1460-1560	200-340	$3/2^+$	1,2	1	****
$\Delta^{++}(1620)$	1590-1610	100-140	$1/2^-$	0,1	0	****
$\Delta^{++}(1700)$	1640-1690	200-300	$3/2^-$	1,2	2	****

$K\pi$ channel

$K^*(700)$	824 ± 30	478 ± 50	0^+	0	0	****
$K^*(892)$	891.66 ± 0.26	50.8 ± 0.9	1^-	0,1,2	1	****
$K^*(1410)$	1414 ± 15	232 ± 21	1^-	0,1,2	1	****
$K_0^*(1430)$	1425 ± 50	270 ± 80	0^+	0	0	****

Fermilab results

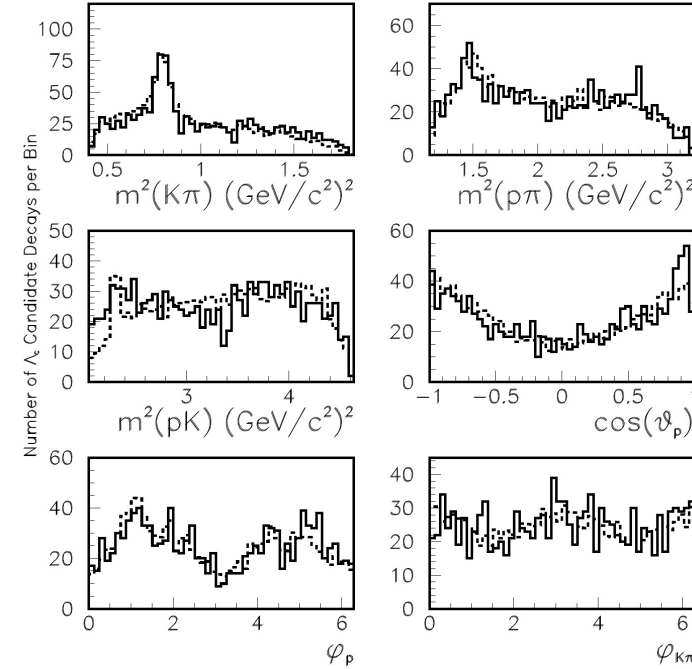
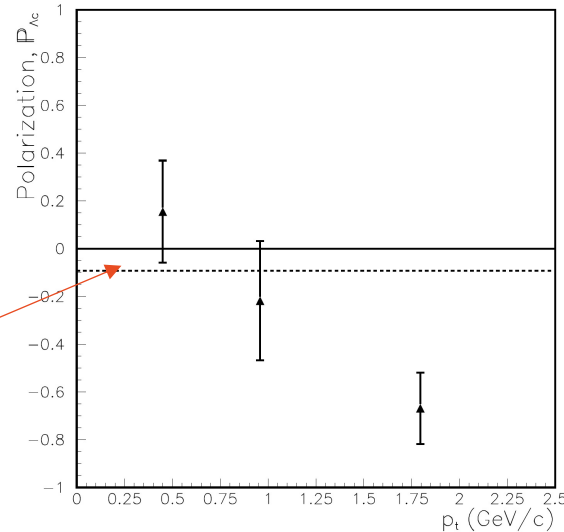
66

Previous analysis from Fermilab

Dataset: 1000 Λ_c^+ events , produced in $\pi - N$ collisions

Result: increasing polarization as a function of p_T

Dashed line:
average
polarization.



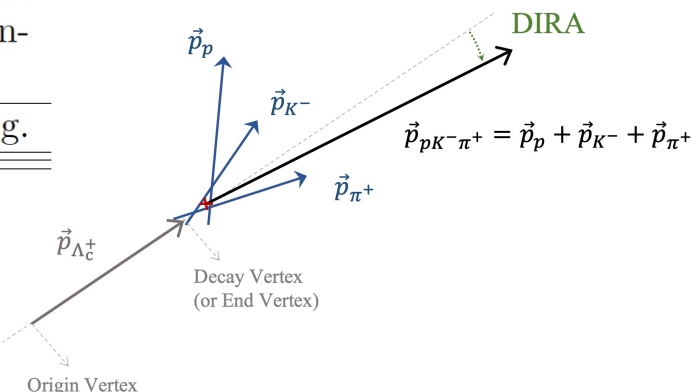
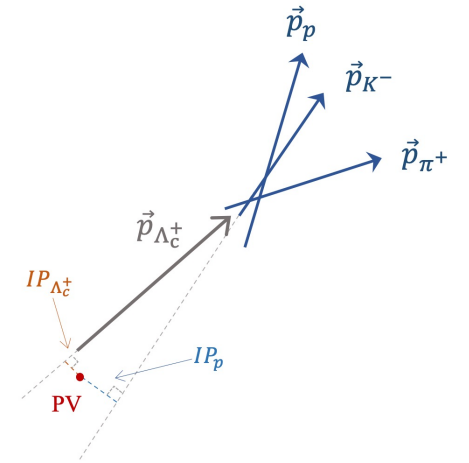
At LHCb: rate of $\bar{c}c$ pairs 0.96 Hz \rightarrow rate of $\Lambda_c^+ \rightarrow p K^- \pi^+$ events ~ 600 Hz

In total, for Run 2 2016, with 4×10^{32} cm⁻²s⁻¹ \rightarrow large number of $\Lambda_c^+ \rightarrow p K^- \pi^+$ events expected

Data sample: $1.7 fb^{-1}$ (2016 only) at a center of mass energy $\sqrt{s} = 13$ TeV

LHCb variables definition

Name	Symbol	Definition
Vertex quality	χ^2_{vtx} or $\chi^2_{\text{vtx}}/\text{ndf}$	χ^2 or χ^2/ndf of the fit of the decay vertex.
Track quality	χ^2_{track}	Quality of the track reconstruction
Ghost probability	$p_{\text{ghost}}(a)$	Probability to be a fake track, coming from a random combination of hits.
Impact Parameter	IP	The transverse distance of closest approach between a particle trajectory and the Primary Vertex (PV), sketched in Fig. 6.2 (right).
	χ^2_{IP}	The change in vertex χ^2 when adding or not a track in the vertex fit.
Direction angle	DIRA	The angle between a line drawn from the PV to the DV of the particle and the sum of the 4-momentum of its decay products, sketched in Fig. 6.2 (left). One typically uses the cosine of the direction angle in selections.
Flight Distance (FD)	χ^2_{FD}	Flight distance of a particle divided by its uncertainty.
PID	$\text{ProbNN}_b(a)$	Probability of the track a of being a particle of type b , where a can be p, K, π, μ, e, d , obtained using a neural network combining the information from sub-detectors.
	$\text{PID}_a(b)$	Same as the probNN variables, without the neural network training.



Selections: HLT2

68

➤ High Level Trigger (HLT)

1. First stage: **HLT1** based on generic track information
2. Second stage: **HLT2** designed to select the three-body decay $\Lambda_c^+ \rightarrow p K^- \pi^+$ specifically

Particle	Selection
Proton	$p > 10 \text{ GeV}/c$ $\text{PID}_p > 5$ $\text{PID}_p - \text{PID}_K > 5$
Kaon	$\text{PID}_K > 5$
Pion	$\text{PID}_K < 5$
All tracks	$p_T > 200 \text{ MeV}/c$ $p > 1 \text{ GeV}$ $\chi_{\text{IP}}^2 > 6$ $\chi_{\text{track}}^2/\text{ndf} < 3$
At least two tracks	$p_T > 400 \text{ MeV}/c$ $\chi_{\text{IP}}^2 > 9$
At least one track	$p_T > 1000 \text{ MeV}/c$ $\chi_{\text{IP}}^2 > 16$
Combination	$2211 \text{ MeV}/c^2 < m < 2543 \text{ MeV}/c^2$ $\sum_{\text{daughters}} p_T > 3000 \text{ MeV}/c$ $\text{acos(DIRA)} < 0.01 \text{ mrad}$ $\tau > 0.15 \text{ ps}$ $\chi_{\text{FD}}^2 > 25$

In general:

- p/p_T requirements to remove combinatorial background
- tracks are required to point away from the PV

(loose) PID selections

Good track-fit quality

Mass window around PDG mass: $m_{\Lambda_c^+} = 2286.46 \pm 0.14 \text{ MeV}$

Lifetime $\tau_{\Lambda_c^+} = (202.4 \pm 3.1) \text{ fs}$

Selections: Trigger

69

- **Hardware trigger L0:** reduce the 40 MHz collision rate to 1MHz.

Select high transverse energy (> 3 GeV) hadrons based on HCAL.

Two *L0 hadron trigger categories*:

1. Triggered On Signal (**TOS**): trigger fired using signal candidates
2. Triggered Independent of Signal (**TIS**) events: signal alone not enough, trigger fired by the rest of the event



In this analysis the two categories are studied separately

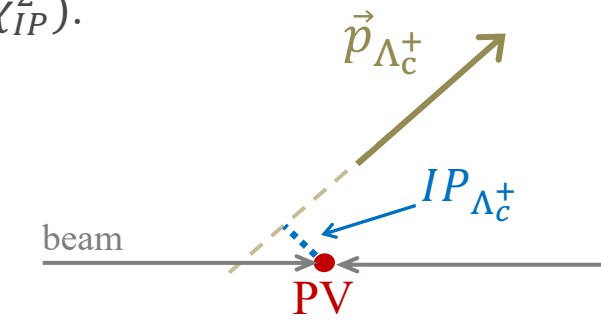
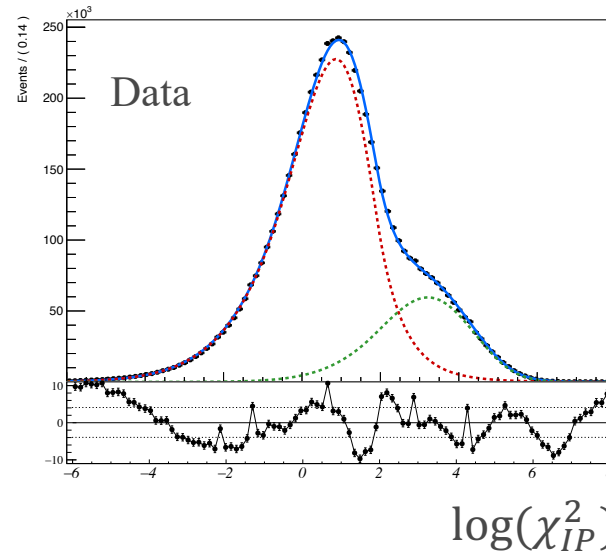
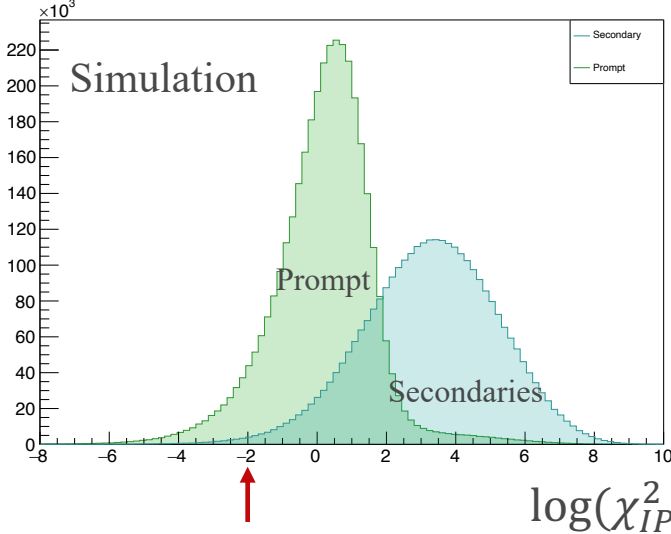
- **Software trigger: High Level Trigger (HLT)**

1. First stage: **HLT1** based on generic track information
2. Second stage: **HLT2** designed to select the three-body decay $\Lambda_c^+ \rightarrow p K^- \pi^+$ specifically

Offline selections

70

- Selection of prompt decays: use the logarithm of the impact parameters $\log(\chi_{IP}^2)$.

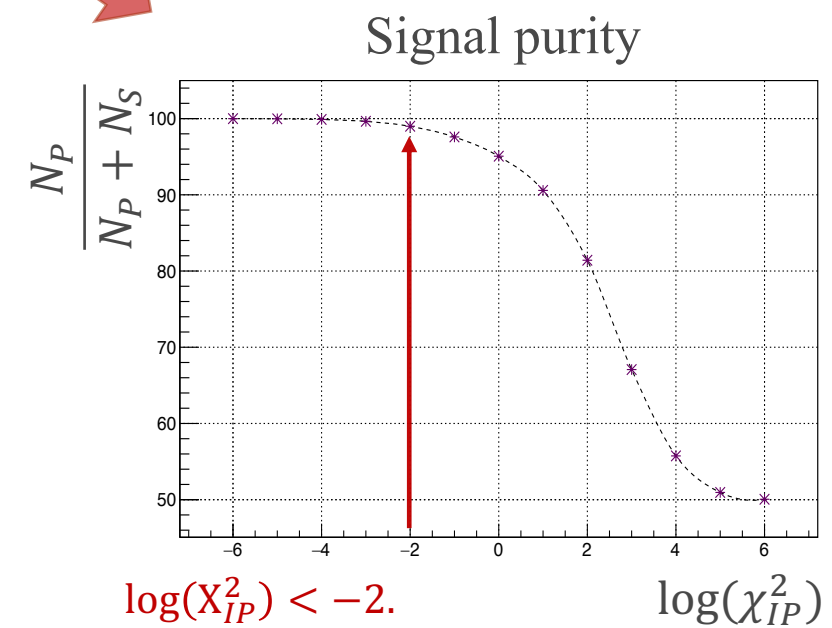


- Use the simulation to constrain the tails in the fit to the data
- Signal purity evaluated in $\log(\chi_{IP}^2)$ the range [-6,6]

Final selection:

$$\log(\chi_{IP}^2) < -2.$$

Prompt signal purity: 98.9 %

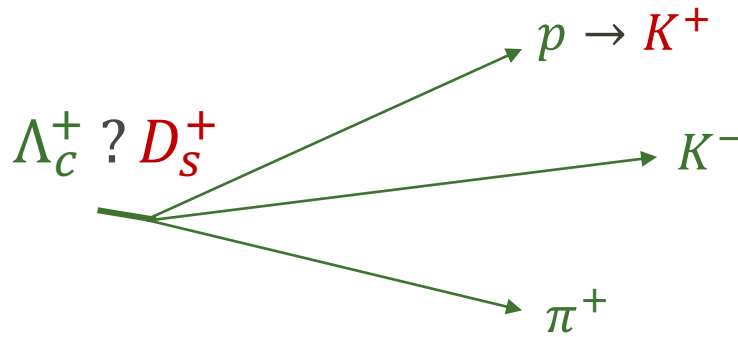


Backgrounds

71

1. Misidentifications: one of the final state particle is wrongly identified
2. Partially reconstructed: 4-body decays with one final particle not reconstructed $X? \rightarrow p K^- \pi^+ Y$
3. Combinatorial background: random combinations of p, K^- and π^+

Example of misidentification:



Such decays will peak outside the mass window, most relevant ones:

$D_s^+ \rightarrow K^+ K^- \pi^+$ with $m_{D_s^+} = 1968.65 \pm 0.07$ MeV

$D^+ \rightarrow K^+ \pi^- \pi^+$ with $m_{D^+} = 1869.65 \pm 0.05$ MeV

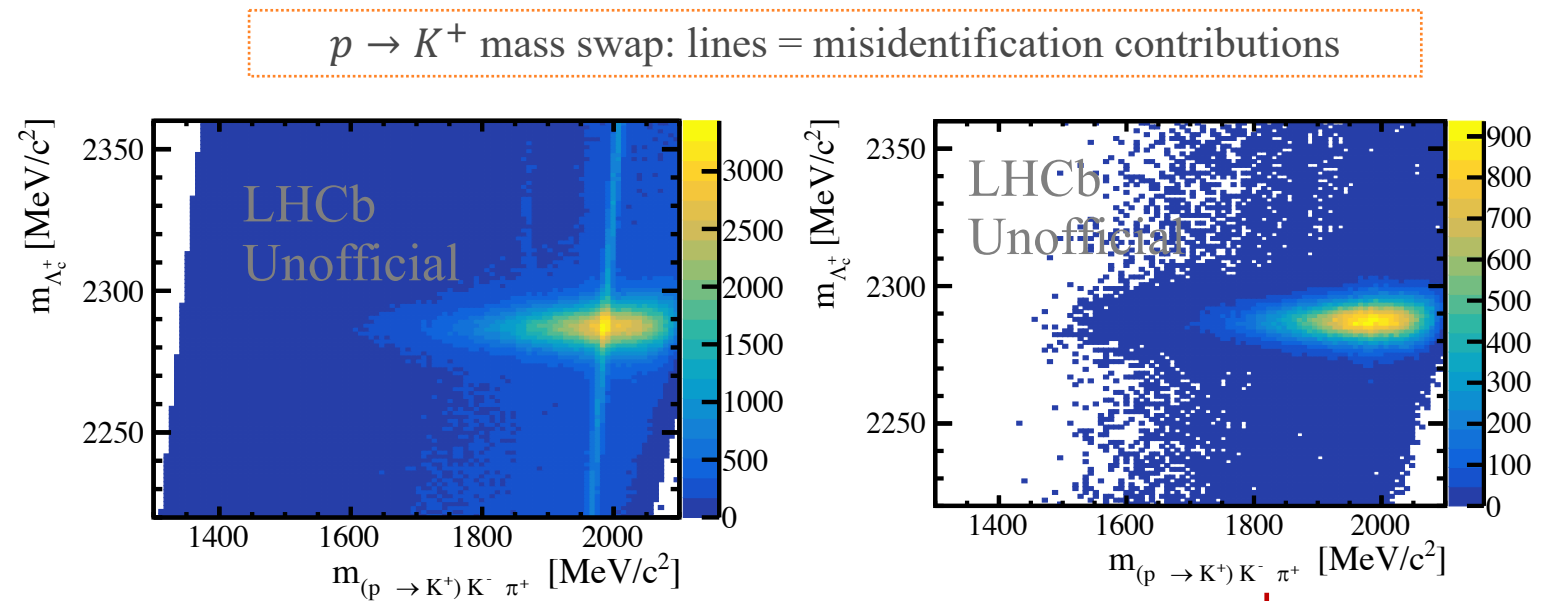
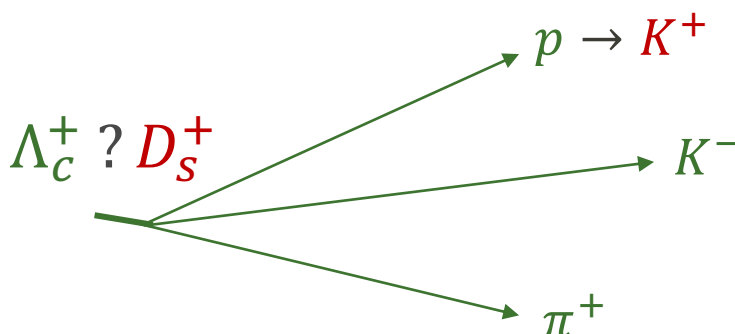
However the tails could contribute to the signal.

Backgrounds

72

1. Misidentifications: one of the final state particle is wrongly identified
2. Partially reconstructed: 4-body decays with one final particle not reconstructed $X? \rightarrow p K^- \pi^+ Y$
3. Combinatorial background: random combinations of p, K^- and π^+

Example of misidentification:



Such decays will peak outside the mass window, most relevant ones:

$D_s^+ \rightarrow K^+ K^- \pi^+$ with $m_{D_s^+} = 1968.65 \pm 0.07$ MeV

$D^+ \rightarrow K^+ \pi^- \pi^+$ with $m_{D^+} = 1869.65 \pm 0.05$ MeV

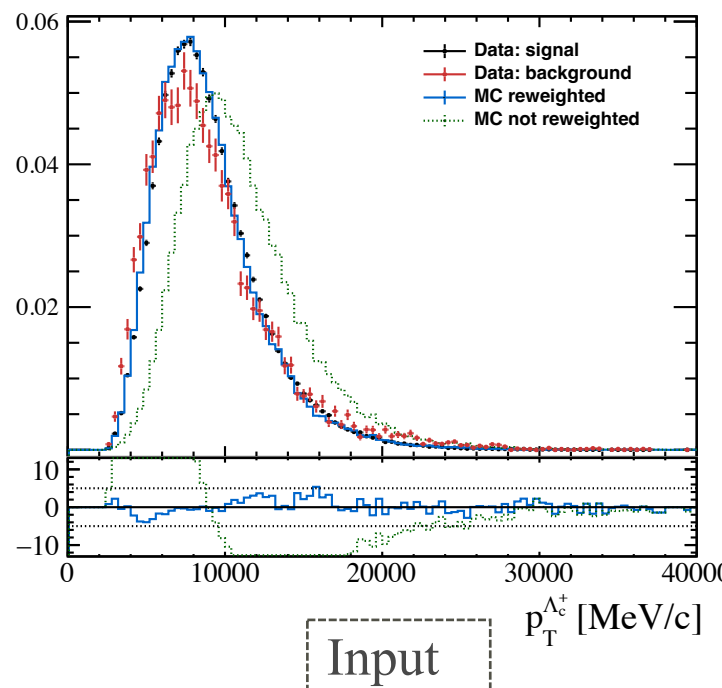
However the tails could contribute to the signal.

After selections: residual contamination < 2 %

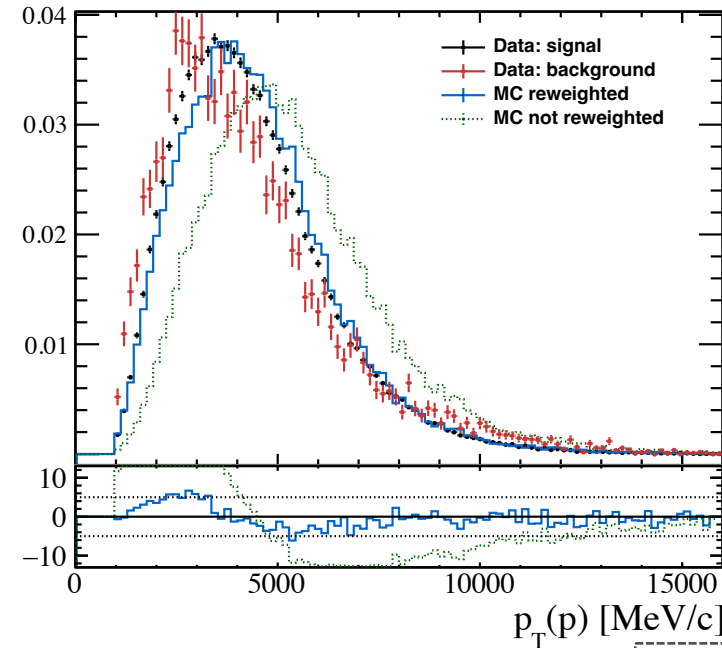
Calibrating the simulation

73

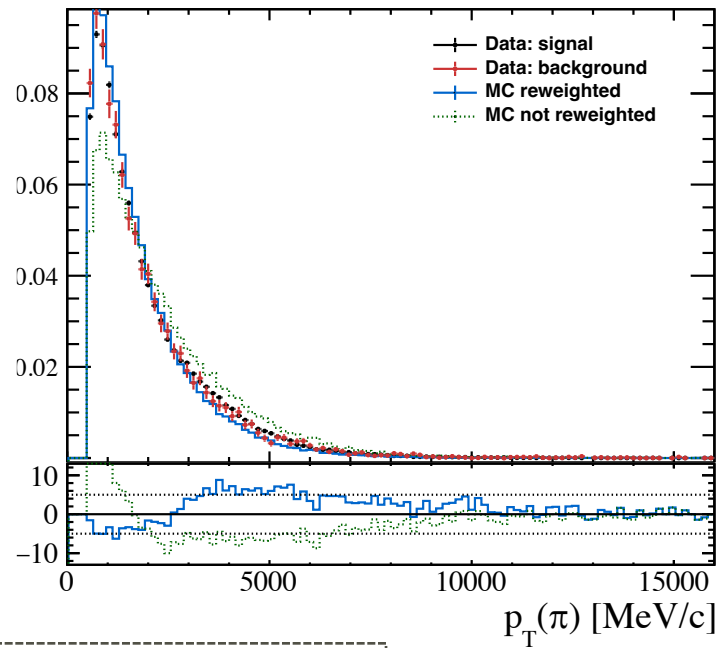
- Simulations is used to include efficiency effects
- However, it is not perfectly reproducing data → **need to correct** it in a **data-driven way**
 - Corrections are applied as *per-event weights*, 3 categories:
 1. L0 trigger
 2. Particle identification (PID)
 3. Kinematics: use machine learning techniques `hep_ml` package, input (Λ_c^+) variables: transverse momentum (p_T), pseudo-rapidity (η), lifetime (τ) and number of VELO tracks ($nTracks$).



Input



Effects on other variables



Effective Alpha

74

Asymmetry parameters for single resonance decays are combination of the helicity couplings, for instance:

$$\alpha_{\Lambda_c}^{\Delta^{++}} = \frac{|H_{1/2,0}^{\Lambda_c^+ \rightarrow \Delta^{++} K^-}|^2 - |H_{-1/2,0}^{\Lambda_c^+ \rightarrow \Delta^{++} K^-}|^2}{|H_{1/2,0}^{\Lambda_c^+ \rightarrow \Delta^{++} K^-}|^2 + |H_{-1/2,0}^{\Lambda_c^+ \rightarrow \Delta^{++} K^-}|^2} = \frac{|F_1|^2 - |F_2|^2}{|F_1|^2 + |F_2|^2}$$

Asymmetry parameters of the Λ_c^+ decay cannot be expressed easily.

Calculate an **effective $\alpha_{\text{effective}}$** using method of M. Davier, et al. Physics Letters B, 306, 3–4, 1993, 411-417

Decompose the amplitude as:

$$\mathcal{P}(\Omega) = f(\Omega) + pg(\Omega) = \hat{f}(\Omega)(1 + p\omega)$$

$$\text{where } \omega = \frac{g(\Omega)}{f(\Omega)}$$

$$\begin{aligned} \mathcal{P}(\Omega) &\propto \underbrace{\left(|\mathcal{A}_{\frac{1}{2}, \frac{1}{2}}|^2 + |\mathcal{A}_{\frac{1}{2}, -\frac{1}{2}}|^2 + |\mathcal{A}_{-\frac{1}{2}, \frac{1}{2}}|^2 + |\mathcal{A}_{-\frac{1}{2}, -\frac{1}{2}}|^2 \right)}_{f(\Omega)} \\ &+ P_z \underbrace{\left(|\mathcal{A}_{\frac{1}{2}, \frac{1}{2}}|^2 + |\mathcal{A}_{\frac{1}{2}, -\frac{1}{2}}|^2 - |\mathcal{A}_{-\frac{1}{2}, \frac{1}{2}}|^2 - |\mathcal{A}_{-\frac{1}{2}, -\frac{1}{2}}|^2 \right)}_{g(\Omega)}. \end{aligned}$$

Second order momenta of f

$$S^2 = \frac{1}{N\sigma^2} = \left\langle \frac{g^2}{f^2}(\Omega) \right\rangle = \int \frac{g^2}{f} d\Omega$$

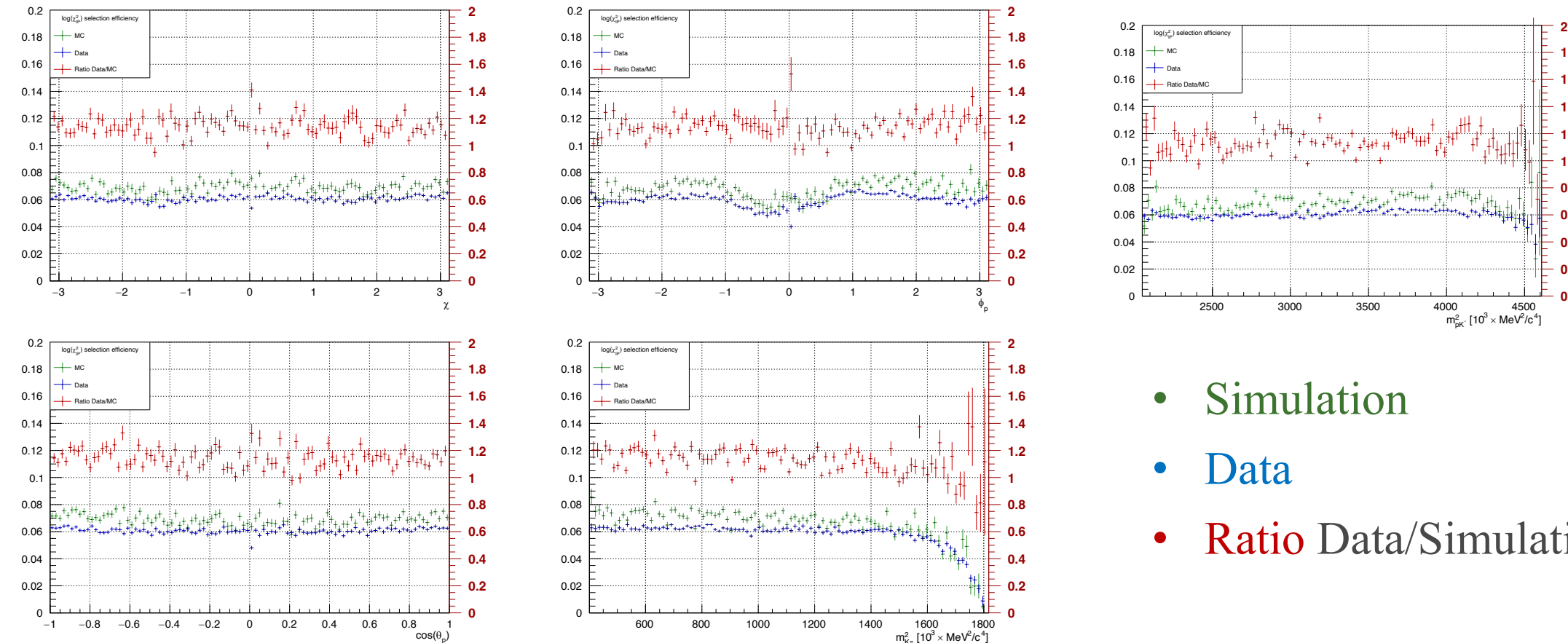
$$S = \frac{2}{\sqrt{3}} |\alpha|$$

Effects of the $\log(X_{IP}^2)$ on the efficiencies

75

The $\log(X_{IP}^2)$ selection introduces a non trivial dependence on efficiencies

Verify that the same effect is present in data and simulation.



- Simulation
- Data
- Ratio Data/Simulation

Misidentifications

76

- All possible misidentifications:

Mis-ID	Final state	Possible decays	BR
$\pi^+ \rightarrow K^+$	pK^-K^+	$\Lambda_c^+ \rightarrow pK^-K^+$	$(1.06 \pm 0.06) \times 10^{-3}$
$K^- \rightarrow \pi^-$	$p\pi^-\pi^+$	$\Lambda_c^+ \rightarrow p\pi^+\pi^+$	$(4.61 \pm 0.28) \times 10^{-3}$
$p \rightarrow \pi^+$	$\pi^+K^-\pi^+$	$D^+ \rightarrow K^-\pi^+\pi^+(\pi^0)$	9.13 ± 0.19 (5.99 ± 0.18)
$p \rightarrow K^+$	$K^+K^-\pi^+$	$D_s^+ \rightarrow K^+K^-\pi^+(\pi^0),$ $D^+ \rightarrow K^+K^-\pi^+$	5.39 ± 0.15 (6.2 ± 0.6), $(9.54 \pm 0.26) \times 10^{-3}$
$p \rightarrow K^+ \&$ $K^- \rightarrow \pi^-$	$K^+\pi^-\pi^+$	$D^+ \rightarrow K^+\pi^-\pi^+,$ $D_s^+ \rightarrow K^+\pi^-\pi^+$	$(5.28 \pm 0.23) \times 10^{-4},$ $(6.5 \pm 0.4) \times 10^{-3}$
$p \rightarrow \pi^+ \&$ $K^- \rightarrow \pi^-$	$\pi^-\pi^+\pi^+$	$D^+ \rightarrow \pi^-\pi^+\pi^+,$ $D_s^+ \rightarrow \pi^+\pi^-\pi^+$	$(3.18 \pm 0.18) \times 10^{-3},$ 1.08 ± 0.04
$\pi^+ \rightarrow K^+ \&$ $K^- \rightarrow \pi^-$	$pK^+\pi^-$	$\Lambda_c^+ \rightarrow pK^+\pi^-$	$(1.11 \pm 0.18) \times 10^{-4}$
$p \rightarrow \pi^+ \&$ $\pi^+ \rightarrow p$	π^+pK^-	$\Lambda_c^+ \rightarrow \pi^+pK^-$	6.28 ± 0.32
$p \rightarrow K^+ \&$ $K^- \rightarrow \pi^- \&$ $\pi^+ \rightarrow K^+$	$K^+K^+\pi^-$	$D_s^+ \rightarrow K^+K^+\pi^-$	$(1.28 \pm 0.04) \times 10^{-4}$

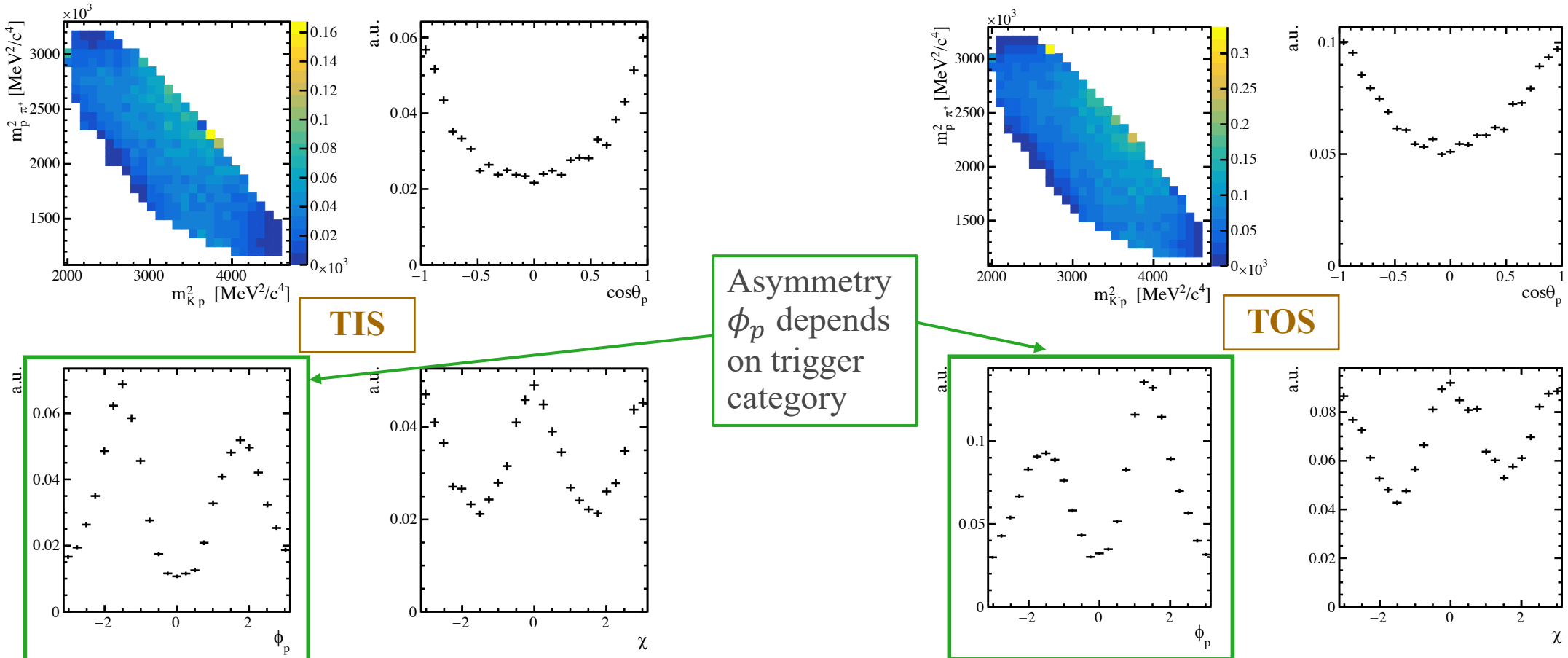
Efficiencies

77

Total efficiency comprises acceptance, selection, trigger, PID and reconstruction:

$$\epsilon_{TOT} = \epsilon_{acc} \times \epsilon_{trigger} \times \epsilon_{sel} \times \epsilon_{PID} \times \epsilon_{rec}$$

Factorize masses (m_{pK^-} , $m_{p\pi^+}$) and angles ($\cos\theta_p$, ϕ_p and χ)

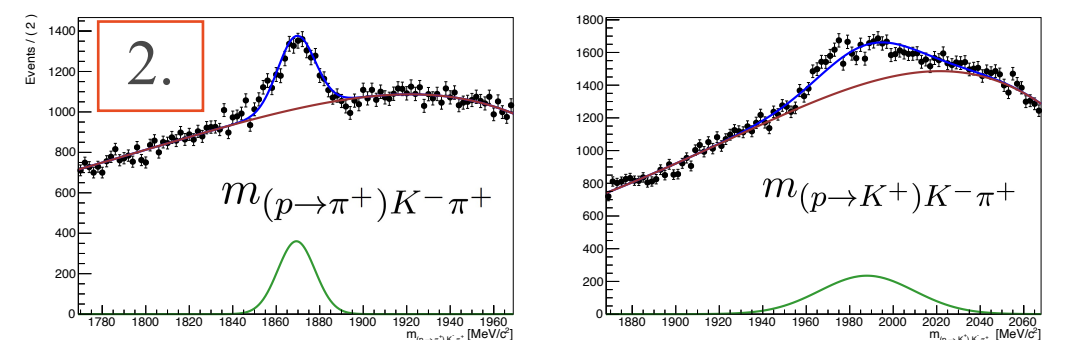
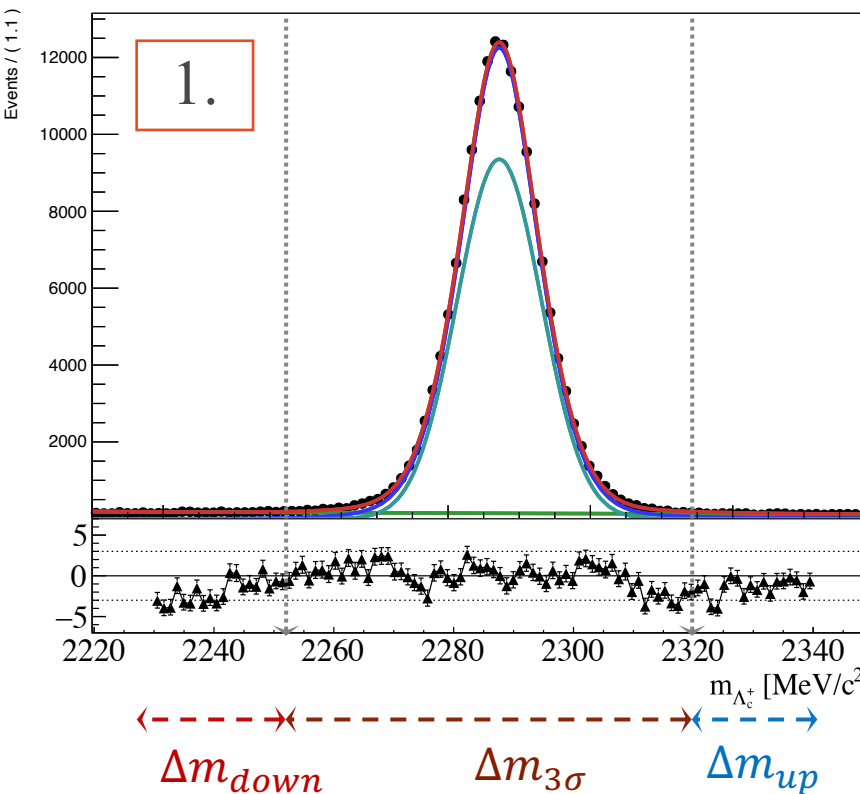


Estimate misidentification residual contribution

78

Estimate the residual contributions:

1. Fit invariant mass to find mean μ and standard deviation σ
2. Pre-fit data with swapped mass hypothesis outside the $\Delta m_{3\sigma}$ window, before selections and after selections
3. Extrapolate the number of residual background in the mass window $\Delta m_{3\sigma}$



$$3. \quad N_{D^+/D_s^+}^{3\sigma} = N_{D^+/D_s^+}^{!3\sigma} \times \frac{\Delta m_{3\sigma}}{\Delta m_{down} + \Delta m_{up}}$$

Trigger	TIS [%]		TOS [%]	
	Mag Up	Mag Down	Mag Up	Mag Down
D^+	0.85	0.90	0.69	0.80
D_s^+	1.37	1.37	1.25	1.35
Λ_c^+	97.23	97.08	97.27	97.11
Background	2.78	2.92	2.73	2.89

Amplitude fit

79

5D unbinned likelihood fit, minimize the negative log likelihood w.r.t. the fit parameters $\vec{\omega}$

Likelihood:

$$-2 \ln \mathcal{L} = -2 \sum_i \ln \mathcal{P}_{sig}(\Omega | \vec{\omega})$$

Include signal weights (sw_i) and drop terms independent of $\vec{\omega}$.

Likelihood is split into two terms running on different samples:

$$-2 \ln \mathcal{L} = -2s_W \sum_i sw_i \ln |\mathcal{M}(\Omega | \vec{\omega})|^2 + 2s_W \ln I(\vec{\omega}) W_{tot}$$

Compute this over data

$$\mathcal{P}_{sig}(\Omega | \vec{\omega}) = \frac{|\mathcal{M}(\Omega | \vec{\omega})|^2 \epsilon(\Omega) \Phi(m_{K^-\pi^+})}{I(\vec{\omega})}$$

Amplitude Efficiency Phase space factor
Normalization integral

$$I(\vec{\omega}) \equiv \int |\mathcal{M}(\Omega | \vec{\omega})|^2 \epsilon(\Omega) \Phi(m_{K^-\pi^+}) d\Omega$$

Efficiency folding

MC integration over simulation,
including efficiency effects

$$I(\vec{\omega}) \propto \frac{1}{\sum_i w_i^{MC}} \sum_i^{N_{MC}} w_i^{MC} |\mathcal{M}(\Omega'_i | \vec{\omega})|^2$$

How are the results changing if a different decision was made?

➤ **Simulation:**

1. Reweighting: change set of input variables
2. L0 trigger: vary the tables within the errors
3. PID correction: use different sample or change the kernel pdf
4. Size of the simulation samples: fit one large toy sample 100 times with different efficiency maps

➤ **Data:**

1. Invariant mass fit: change model
2. Model choice: generate with alternative models (M10 and M21) and fit with nominal model
3. Change values of masses and widths of known resonances

➤ **Fit machinery:**

Generate 1000 toys, fit it. Compare the result with input value for each fit parameter.